Alma Mater Studiorum - Università di Bologna

SCUOLA DI SCIENZE

Dipartimento di Chimica Industriale“Toso Montanari”

Corso di Laurea Magistrale in

Chimica Industriale

Classe LM-71 - Scienze e Tecnologie della Chimica Industriale

How important are H…H intermolecular interactions in single crystals of distyrylbenzene derivates?

Tesi di laurea sperimentale

CANDIDATO

Filippo Vacchi

RELATORE

Prof. Andrea Mazzanti

CORRELATORE

Prof. Frank Blockhuys

Dott. Léon Luntadila Lufungula

Anno Accademico 2022-2023

Abstract

L'ingegneria dello stato cristallino è una disciplina in rapida evoluzione che comprende vari rami della chimica come la chimica computazionale, la cristallografia, la chimica organica e tante altre scienze quali alcune branche della biologia. Come disciplina trova in particolare applicazioni nell'ambito hi-tech per lo studio ad esempio di semicoduttori o in ambito farmaceutico per studi di farmacocinetica e solubilità.

In questo contesto si inserisce lo studio dei cristalli organici di distirilbenzene, la cui utilità è già comprovata come semiconduttore, nella costruzione di sistemi OLED o per applicazioni nel campo della sensoristica.

Usando quindi un approcio ingegneristico, si vuole valutare la possibilità di migliorare le proprietà di questi materiali con modifiche chimiche, in modo da esaltarne le proprietà chimico fisiche desiderate. Queste ultime sono indissolubilmente in relazione con l'impaccamento cristallino che dipende a sua volta dalle interazioni intermolecolari. La conoscenza delle interazioni intermolecolari è quindi essenziale per la comprensione delle strutture cristalline.

Durante il mio periodo di preparazione della tesi, presso l'università di Anversa, nel gruppo di ricerca del professor Frank Blockhuys, ho studiato diverse strutture cristalline basate su uno scheletro di distirilbenzene in cui gli idrogeni sugli anelli aromatici vengono sostituiti in modo simmetrico da gruppi metossi come visibile in figura 1.

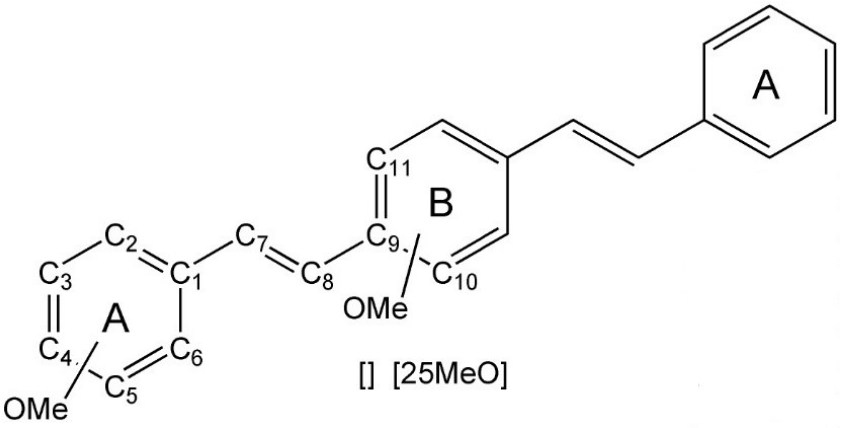

Figure 1: Struttura base delle molecole di distirilbenzene studiate

Nonostante la presenza di questi gruppi però si è osservato, attraverso esperimenti computazionali, che oltre a interazioni intermolecolari di tipo C-H...O, prevedibili per l'inserimento di eteroatomi nella struttura, sono presenti in modo ubiquitario interazioni intermolecolari di tipo C-H...H.

Questo tipo di interazioni rappresentano ancora oggi un argomento molto controverso nella comunità scientifica che dibatte sia dell'esistenza dell'interazione come forza di legame debole che della teoria alla base, utilizzata per l'identificazione dell'interazione. Nonostante tali controversie, questo genere di interazione rimane ancora oggi poco investigata e per questa ragione si è deciso di approfondire l'argomento.

L'obbiettivo dell'attività condotta durante il tirocinio è stato lo studio, la caratterizzazione e infine la classificazione in tre diverse categorie delle interazioni intermolecolari di tipo C-H...H. Ciò è stato possibile grazie allo svolgimento di diversi calcoli e alla selezione delle strutture adatte per studi più approfonditi. Le interazioni sono state categorizzate usando come parametri il numero di atomi coinvolti, la forma dell'interazioni e altre variabili come la densità elettronica e la curvatura della linea di interazione.

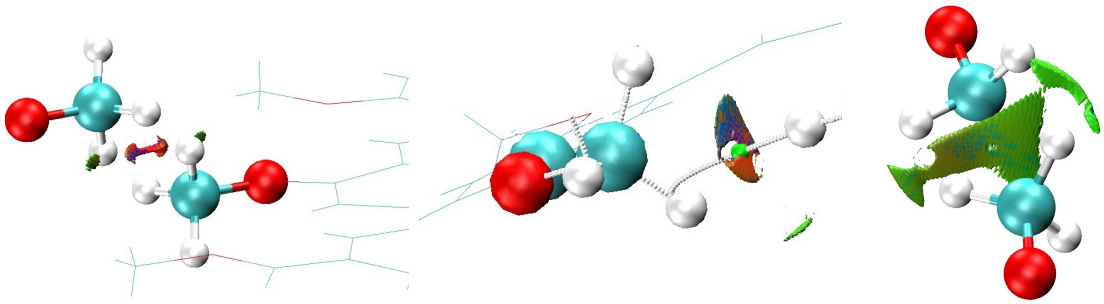

Figure 2: Le tre differenti categorie di interazione C-H...H intermolecolari individuate

Oltre che per lo studio e la comprensione delle strutture cristalline di distirilbenzene, studi futuri su questo tipo di interazioni potrebbero essere essenziali per la comprensione generale delle strutture cristalline, ma potrebbero anche aprire la strada per la spiegazione di fenomeni chimici come il meccanismo di self assembly.

Abstract (ENG)

Crystal engineering is a fast-developing discipline encompassing various branches of chemistry such as computational chemistry, crystallography, organic chemistry and many other fields that may also involve branches of biology. As a discipline, it has particular applications in the hi-tech field for the study of, for example, semiconductors or in the pharmaceutical field for pharmacokinetic and solubility studies.

This includes the study of organic distyrylbenzene crystals, whose utility is already proven as a semiconductor, in the construction of OLED systems or for applications in the field of sensor technology.

Using an engineering approach, the aim is to assess the possibility of improving the properties of these materials by means of chemical modifications, to enhance the desired chemical and physical properties, which are inextricably linked with the crystalline packing, which in turn depends on intermolecular interactions. The knowledge of intermolecular interactions is, therefore, essential for understanding crystal structures.

During my thesis preparation at the University of Antwerp, in the research group of Professor Frank Blockhuys, I studied several crystal structures based on a distyrylbenzene skeleton in which the hydrogens on the aromatic rings are symmetrically replaced by methoxy groups as visible in Figure 3.

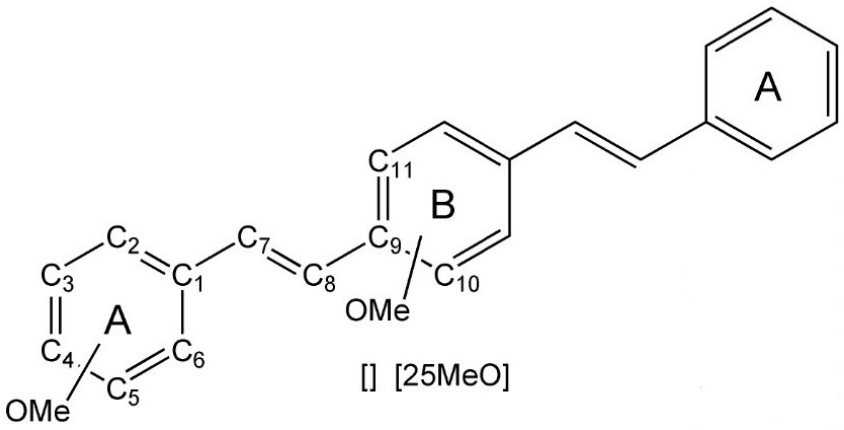

Figure 3: back-bone structure of the molecules of distyrylbenzene molecules

Despite the presence of these groups, however, it has been observed through computational experiments, that in addition to C-H...O type intermolecular interactions, which can be expected due to the inclusion of heteroatoms in the structure, C-H...H type intermolecular interactions are ubiquitously present.

These types of interactions are still a highly controversial topic in the scientific community, which debates both the existence of the interaction as a weak bonding force and the underlying theory used to identify the interaction. Despite the controversy, however, this type of interaction still remains under-investigated and for this reason it was decided to investigate the topic further.

The aim of the activity carried out during the training was to study, characterize and finally classify intermolecular interactions of the C-H...H type into three different categories. This was achieved by carrying out various computations and selecting suitable structures for further study. The interactions were categorized using the number of atoms involved, the shape of the interaction and other variables such as electronic density and the curvature of the interaction line as parameters.

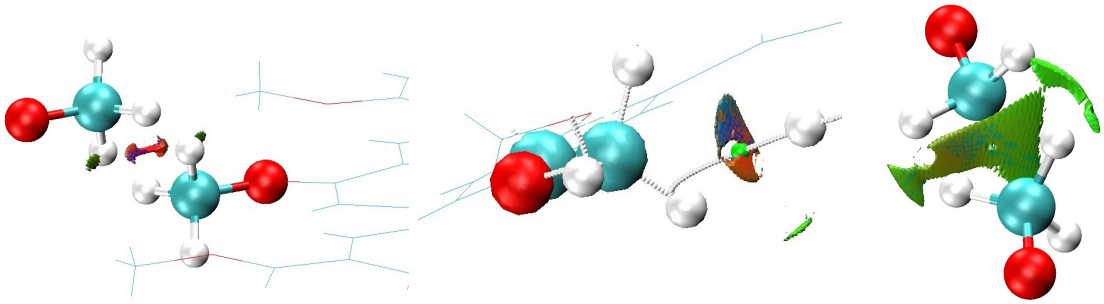

Figure 4: three different types of C-H...H interactions identifyed

In addition to the study and understanding of distyrylbenzene crystal structures, future studies on this type of interaction could be essential for the general understanding of crystal structures, but could also pave the way for the explanation of chemical phenomena such as the self-assembly mechanism.

Contents

1 Introduction

1.1 Crystal engineering

Crystal engineering [1][2] is an interdisciplinary field of chemistry focused on understanding intermolecular and intramolecular interactions in order to design solid structures with innovative properties and behaviour. It also allows to build predictive models to derivate the chemical-physical properties of the crystals; this approach that combine traditional chemistry with crystallography studies and computational chemistry is very useful to investigate any type of crystals from organic based to inorganic ones.

As a discipline, it has various applications in the pharmaceutical industry[3], where it is related to drug kinetics[4] and studies of solubility in organic tissues[5]. It also finds applications in the field of liquid crystals display technology, semiconductors, and next-generation sensors[6].

Historically, the origin of this research topic is around 1960, but only around 1980 and 1990 there have been an incredible evolution of the discipline thanks to the evolution of the computational chemistry and the progresses in the computer science. Moreover, in the same period the "Cambridge structure database" was founded, as an archive that collects an increasing number of crystal structures, a useful instrument for statistical analysis and for the development of predictive models.

In this thesis is presented the analysis of crystal structures of a class of compounds in order to future studies of their chemical physical properties through the investigation of the different classes of intermolecular interactions.

In the end it may be possible to synthetize and crystallize new molecules, so in other word to design a new structure with specific properties using the knowledge acquired from the study of the same class of molecular crystals.

1.2 Uses of distyrylbenzene-based materials

The application of organic crystals in the technological industry is every year more and more important, they can have many applications in various fields of pharmaceutical and hi-tech industry.

A molecular crystal is a type of crystalline solid composed of individual molecules held together by intermolecular forces[7]. Unlike ionic crystals or metals, where the constituents are ions or metal atoms, respectively, molecular crystals are made up of discrete, covalently bonded molecules. These molecules are typically held together by weak forces such as Van der Waals forces, hydrogen bonds, or dipole-dipole interactions.

In a molecular crystal, the molecules are arranged in a regular, repetitive pattern throughout the crystal lattice. The arrangement of molecules in the lattice determines many of the material's physical properties, including its melting point, hardness, and electrical conductivity.

The materials based on distyrylbenzene (DSBs) crystal structures, in particular find applications because of their semiconductors properties in optoelectronic devices, for the construction of organic light-emitting devices (OLED)[8][9], as memory and non-linear optical (NLO) materials [10][11] or as gas- or ion- selective sensors[12].

In order to improve these important properties such as the efficiency of light emission, useful for example for displays and screens, various strategies to modify the structure have been developed in this thesis. It could be possible for example to lower the barrier to electron injection by increasing the electron affinity of the materials, this can be performed by substituting the DSB backbone with electron-withdrawing heteroatoms as the nitrogen of pyrazine ring[13][14].

The properties of these materials are strictly connected with the solid state structure of the molecules investigated, in particular with the crystal packing, for this reason the use of crystal analysis as XRD (x-ray diffraction) and the computational experiments are central for the comprehension of the behaviour of the materials and for the development of models using data analysis and statistical instruments.

For this work have been considered a specific class of crystal structures based on distyrylbenzenes (DSBs) (Fig.5) with a symmetrical distribution of methoxy groups around the central and peripheral benzene rings, the number of methoxy groups on the external rings varies from 1 to 3 whereas on the central ring there may be no methoxy groups or 2.

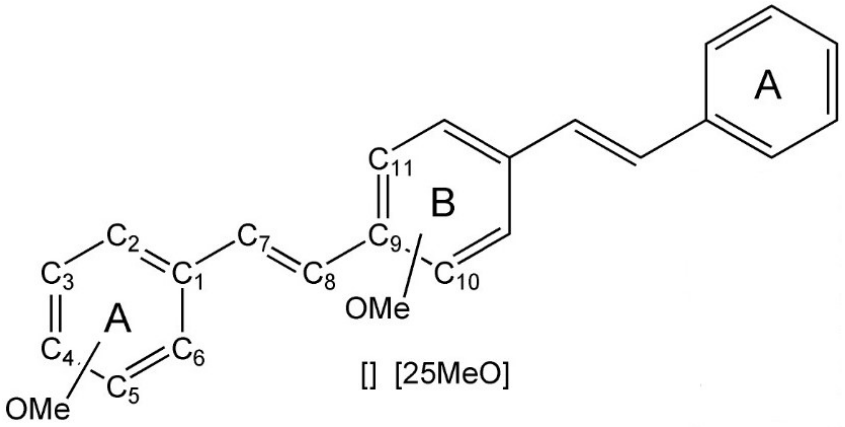

Figure 5: back-bone structure of distyrylbenzenes (DSBs) molecules

Since the technological applications of organic materials are invariably based on their solid state, it is clear that apart from their molecular properties, their bulk properties are of great importance. In turn, these bulk properties depend on the three-dimensional organization of the molecules in the crystal that is partially determined by intermolecular interactions[14].

In this way, the understanding of weak intermolecular interactions as CH-O, CH-π and CH-H is central for the study and the following manipulation of the crystal structure. For the apparent great importance in the crystal packing and for the lack of presence of the topic in the recent scientific literature, have been decided to focus the study on a specific intermolecular interaction, the CH-H interactions.

1.3 State of the art

As cited in the previous chapter, the topic of C-H...H interaction is still very controversial in the scientific literature for two reasons: the first is not properly related with the specific type of interaction but with the basic concepts of the QTAIM theory, while the second reason is directly related with the interaction and considers inconsistent the experiments done.

In this controversy, there are two parts that summarize the opposite opinions, the first is represented by *Cherif F. Matta, Jesus Hernandez Trujillo et al.* that support the existence of the C-H...H interaction; the second part is represented by *Jordi Poater, Miquel Solà et al.* that criticize the presence of this driving force and the utility of the QTAIM theory.

In the articles published by *Matta et al.* the authors analysed systems of condensed benzene rings where intramolecular C-H...H interactions are present as shown in figure 6, from article [15].

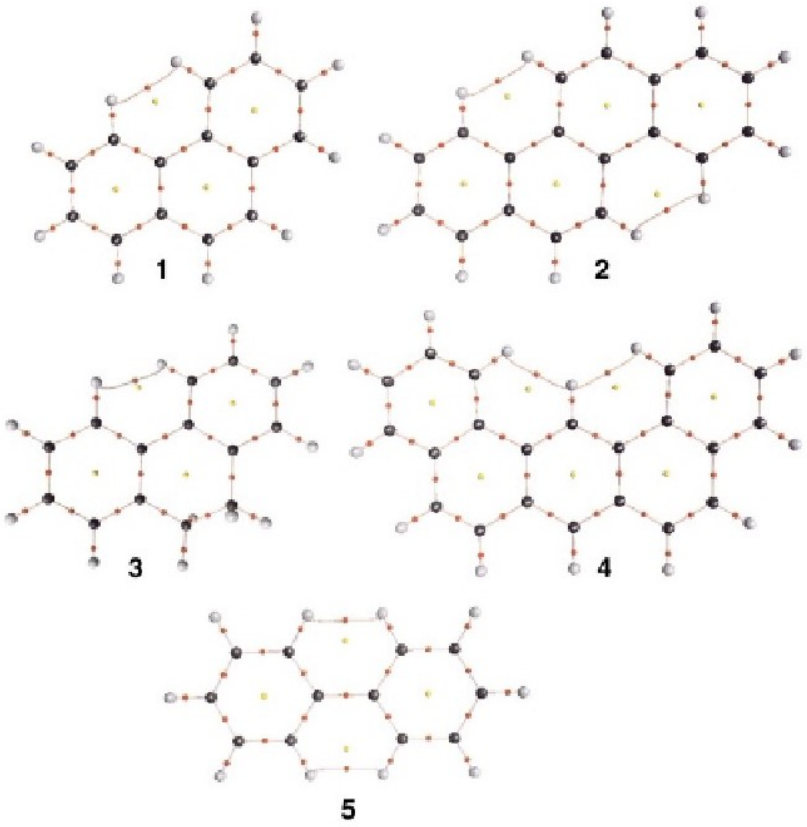

Figure 6: Molecular graphs for phenanthrene (1), chrysene (2), 9,10-dihydrophenanthrene (3), dibenz[a,j]anthracene (4), and planar biphenyl (5). Bond critical points (CPs) are red, ring CPs yellow [15]

In the article is highlighted the existence of a C-H...H interaction between hydrogens with the same charge moreover not only it was found with DFT calculation that identified the critical points, but also the authors sustained that it represent a stabilization energy for the system thanks to decomposition computational experiments. In particular, the stabilization energy for the C-H...H interaction is approximately of 5 Kcal/mol for phenanthrene, chrysene, and dibenz[a,j]anthracene and for the other molecules this stabilization force is between 10 and 20 Kcal/mol.

On the other hand, this article has been criticized by *Poater et al.*, in their article [16]. In particular, they sustained that the C-H...H interaction in biphenyl molecule is not a bonding interaction, but is a Pauli repulsive force. These conclusions were reached by analysing the potential energy surface (PES) and the molecular orbital (MO) model instead of the atoms in molecules theory (AIM).

The debate about this subject continued [17][18] without finding a real solution that explained in unambiguous way the interaction. For this reason we have been decided to investigate this particular topic. To this aim in this work of thesis we use the model of Quantum theory of atoms in molecules (QTAIM theory), whose main concepts will be explained in the next chapter.

1.4 Quantum theory of atoms in molecules

To unambiguously locate the presence of a bonding interaction, we can perform a calculation based on the Quantum Theory of Atoms In Molecules (QTAIM) by R. F. W. Bader[19]. This theory states that the chemical structure of a system can be completely and unambiguously determined by investigating the topology of the electron density distribution $\rho(\mathrm{r})$.

The topology of the electron density distribution in a molecular system is the physical manifestation of the forces acting within the system. Dominant among these is the attractive force exerted on the electrons by the nuclei, resulting in an accumulation of electronic charge near the nuclei. Therefore, local maxima appear in the electron density distribution at the position of the nuclei, as shown in figure 7 for an ethylene molecule.

Apart from the maxima at the nuclear positions, we can also distinguish the presence of saddles between the carbon nuclei, and between each carbon nucleus and its associated hydrogen nuclei. Moreover, every pair of nuclei which are linked by (what we consider) a chemical bond will display such a saddle structure in the electron density region between the nuclei.

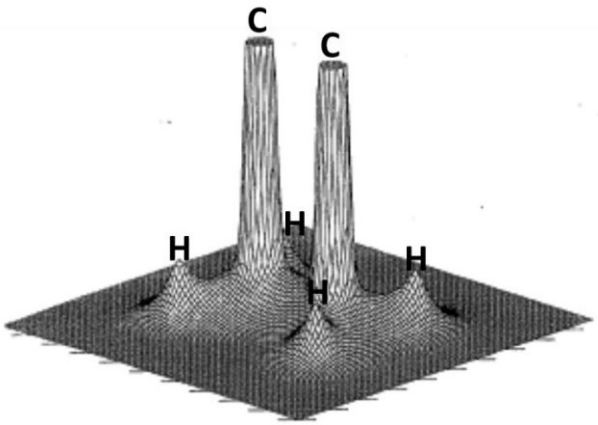

Figure 7: Relief plot of the electron density distribution of ethylene in the plane of the molecule. The maxima associated with the carbon nuclei are much larger than those associated with the hydrogen nuclei. Therefore, the carbon peaks are truncated to display both types of maxima. Adapted from Atoms In Molecules: A Quantum Theory by R. F. W. Bader[19]

Every topological feature of $\rho(\mathrm{r})$, whether it be a maximum, a minimum, or a saddle, has associated with it a point in space called a critical point where the first derivatives of $\rho(\mathrm{r})$ vanish, i.e., the gradient $\nabla\rho$ becomes equal to zero. Whether a function f(x) is in a maximum or a minimum at an extreme is determined by the sign of its second derivative at that point.

The second derivative is also called the curvature of a function f(x) and can be defined as the limiting difference between its two first derivatives or tangent lines which bracket that point,

as depicted graphically in figure 8. At a point where the function is a minimum, the second derivative is the difference between a positive and a negative slope and is, therefore, greater than zero, while, at a maximum the second derivative is the difference between a negative and a positive slope and the result is a value less than zero.

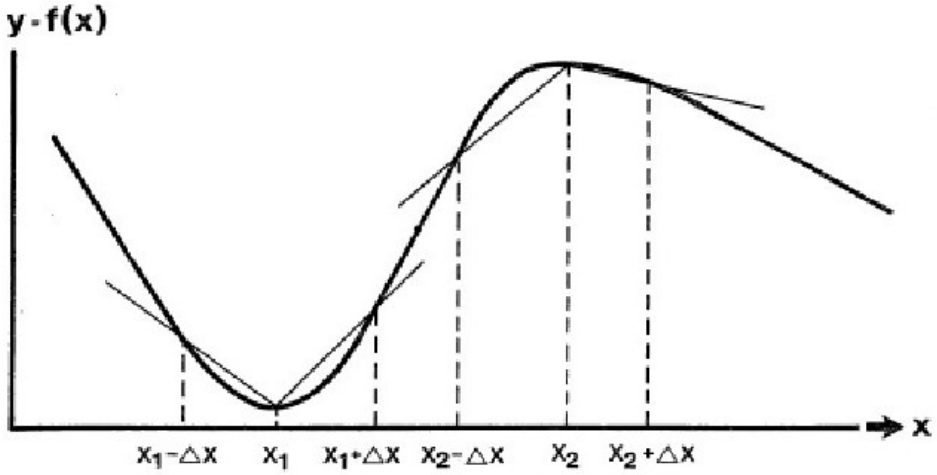

Figure 8: Definition of curvature as the limiting difference ($\Delta x \rightarrow 0$) in the tangent lines which bracket a given point. At x1 where f(x) is a minimum, the curvature is positive, whereas at x2, where f(x) is a maximum, the curvature is negative.

For an arbitrary choice of coordinate axes, one will encounter nine second derivatives of the form $\theta 2\rho/\theta x \theta y$ in the determination of the curvature of ρ at a point in space. Their 3×3 array is called the Hessian matrix of the charge density, or simply, the Hessian of ρ. This matrix can be diagonalized, by solving the corresponding eigenvalue problem which constitutes finding a rotation of the coordinate axes towards the principal axes to reduce all off-diagonal elements to zero. As a result, only the three second derivatives of ρ with respect to the principal axes remain in the diagonalized Hessian. For example, the principal axes in the critical point of the carbon–carbon bond of ethylene (Figure 3) consist of the axis along the carbon–carbon bond path and two axes perpendicular to the bond path.

The second derivatives along these principal axes are the eigenvalues of the Hessian matrix and the sum of these eigenvalues is called the Laplacian of ρ, denoted as $\nabla 2\rho$. The Laplacian is a very important property, as it determines where electron density is locally concentrated and depleted.

Critical points can be classified into four groups depending on the signs of the eigenvalues of the Hessian matrix, i.e., the curvatures along the principal axes. We define the rank of a critical point, denoted by ω, as the number of non-zero eigenvalues of the Hessian of ρ. The signature,

denoted by σ, is the algebraic sum of the signs of the eigenvalues, with a positive eigenvalue corresponding to +1 and a negative eigenvalue corresponding to -1. The critical point is then labelled by its combination of rank and signature (ω, σ). With relatively few exceptions, the critical points of charge distributions for molecules at or in the neighbourhood of energetically stable geometrical conformations are all the rank three, resulting in four possible combinations of rank and signature as shown in table 1.

(ω,σ)	Type	Explanation
(3, -3)	Nuclear	All curvatures are negative and ρ is a local maximum.
(3, -1)	Bond	Two curvatures are negative and ρ is a maximum in the plane defined by their corresponding axes, while ρ is a minimum along the remaining axis which is perpendicular to this plane. The axis with the positive curvature (the internuclear axis) is parallel to the bond path, while the plane with the two negative curvatures (the interatomic surface) is perpendicular to it, as seen for the carbon–carbon bond in Figure 7.
(3, +1)	Ring	Two curvatures are positive and ρ is a minimum in the plane defined by their corresponding axes. ρ is a maximum along the third axis which is perpendicular to this plane
(3, +3)	Cage	All curvatures are positive and ρ is a local minimum

Table 1: Critical point types, defined by their rank and signature.

Figure 9 shows the visualization of a QTAIM analysis performed on a cubane molecule (C8H8) and displays all four types of critical points. Nuclear critical points (NCPs) define the positions of maxima in the electron density corresponding to the different nuclei in the system. Bond critical points (BCPs) define the positions of saddles in the electron density and have a corresponding bond path which connects the BCP to the NCPs of the nuclei participating in the bonding interaction.

The molecular graph is defined as the union of the closures of the bond paths, displaying the system's connectivity. Ring (RCPs) and cage critical points (CCPs) show the presence of, respectively, ring and cage structures, but are less important to the goals of this work and will be disregarded from now on.

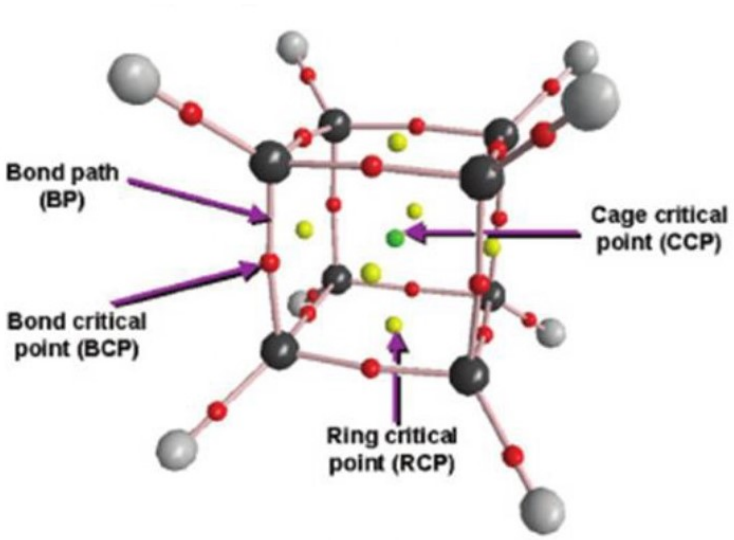

Figure 9: Molecular graph of cubane showing the bond paths (pink lines) and all four critical point types: nuclear (color- coded by element: C black sphere, H grey sphere), bond (red sphere), ring (yellow sphere) and cage (green sphere). Adapted from An Introduction to the Quantum Theory of Atoms In Molecules by C. F. Matta.

The value of ρ at a BCP will be an indication of the strength of the interaction, as more electron density in the internuclear region will result in a stronger bond. The sign and value of $\nabla 2\rho$ will be indicators of the nature of the bond and the bond strength. As $\nabla 2\rho$ is the sum of the three principal curvatures, it will be the result of two competing processes: the perpendicular contractions of ρ towards the bond path (due to the negative curvatures) which leads to a concentration of charge along this bond path, and the parallel expansion of ρ away from the interatomic surface (due to the positive curvature) which leads to its separate concentration at each of the nuclei. When $\nabla 2\rho < 0$ and is large in magnitude, ρ(r) is also large, and electronic charge is concentrated in the internuclear region as a result of the dominance of the perpendicular contractions of ρ towards the bond path. When $\nabla 2\rho > 0$, ρ is relatively low in value and electronic charge is depleted from the internuclear region and contracted towards each of the separate nuclei. This makes the QTAIM theory very powerful for studying and classifying bonds. Interactions with large values of $\nabla 2\rho$ will be easily classified, but care must be taken when classifying interactions with values of $\nabla 2\rho$ close to zero, as they form a transit region with characteristics somewhere in between those of the shared-shell and closed-shell limits.

1.5 Self assembly technology

One of the possible application of the C-H...H interactions in future studyes is in the development of models that can explain the chemical auto assembly mechanism.

Auto-assembly in chemistry typically refers to the process that involve molecules or nanoscale structures which spontaneously organize themselves into a specific patterns or arrangements without external guidance or intervention. This phenomenon is usually observed in systems containing molecules or particles with complementary shapes, sizes, or chemical properties.

One common example of auto-assembly is the formation of micelles in solutions of surfactant molecules. Surfactants have a hydrophilic (water-attracting) "head" and a hydrophobic (water-repellent) "tail." When these molecules are dispersed in water, they can spontaneously form micelles, which are spherical structures where the hydrophilic heads are on the outer surface, interacting with water, and the hydrophobic tails are sequestered in the interior away from water.

Another example is the self-assembly of lipid molecules in biological systems. Lipids, which are components of cell membranes, can spontaneously form bilayer structures in aqueous environments. This self-assembly property is crucial for the formation and stability of cell membranes.

In the context of nanotechnology, researchers often exploit the principles of auto-assembly to create functional nanomaterials and devices. For instance, certain nanoparticles can self-assemble into well-defined structures, which is essential in the development of nanoelectronics, sensors, and drug delivery systems.

Auto-assembly processes are driven by various forces, including van der Waals forces, hydrogen bonding, hydrophobic interactions, and electrostatic forces, in this context the investigation of a new type of intermolecular interaction could be useful in order to have a complete knowledge of the phenomenon.

2 Aim of the project

Because of the important role of intermolecular interactions in crystal structures, it's quite easy to understand our interest in every unusual and controversial intermolecular interaction, that in this case is represented by C-H...H intermolecular interactions. In the structure studied they appeared to be an important and ubiquitous interaction and sometimes also the main driving force for the crystal packing.

The aim of the project is the identification and characterization of this intermolecular interaction using computational simulations in order to understand the role of this interaction in the crystal packing. Thanks to these calculations, it has been possible to identify 3 types of C-H...H intermolecular interactions. In the end the research made possible the revaluation of an unexplored interaction and lets us speculate about its importance not only for crystal packing but also for fields as the auto assembling technology.

During my thesis period, thanks to Erasmus+ project, I worked in Prof. Blockhuys' group in the Department of Chemistry of the University of Antwerp (Belgium) on the study of crystal structures of a collection of symmetric distyrylbenzene compounds with a variable number and disposition of methoxy groups in the central and external rings in order to identify and study the intermolecular interactions. The collection of structures consisted of 23 crystal structures, 18 of them were already used for other studies and 5 were found in the CSD database.

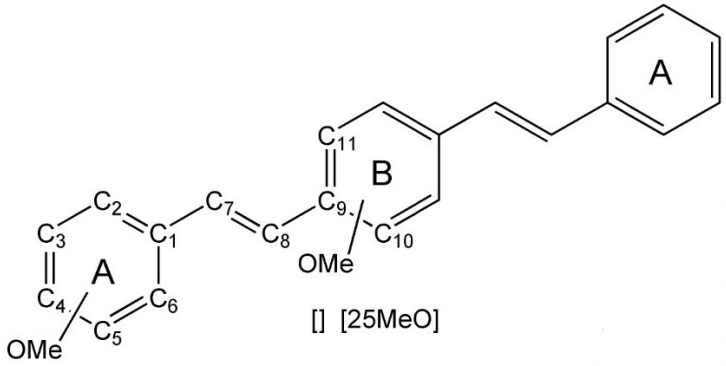

Figure 10: back-bone of distyrylbenzenes (DSBs) structure with derivations

Within these 23 compounds, our attention has been focused on the analysis of two specific structures: (E,E)-1,4-bis(2-(2,4,6-Trimethoxyphenyl)ethenyl)-2,5-dimethoxybenzene (from CSD database "BEZYAH") and (E,E)-1,4-bis(2,3,4-trimethoxystyryl)-2,5-dimethoxybenzene, which structure is shown in the image below (Fig.11), because of the strength of their intermolecular

C-H...H interactions and for the considerable number of them. Moreover were performed "NCI" plot calculations of every C-H...H interaction, in order to understand better their function and the atoms involved.

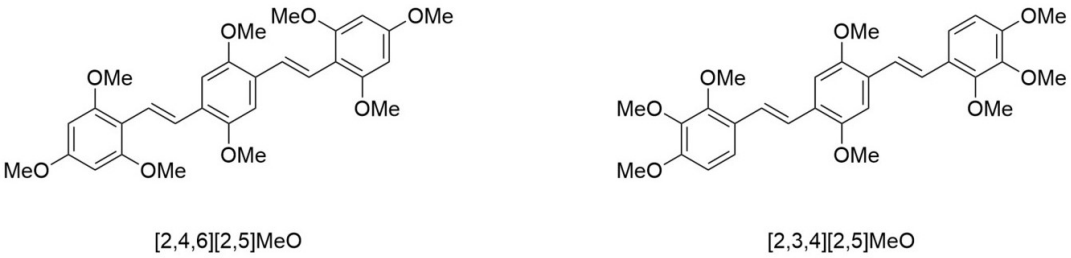

Figure 11: structure selected

The aim of the project is to study and categorize the CH...H interactions. By reaching this point, it could be possible to understand the crystal packing and maybe in the future also to explain phenomenon as the auto assembly mechanism.

Distyrylbenzenes (DSBs) crystal structures are highly suitable for electronic industry as opto-elctronic materials in this field is very important the crystal packing of the molecules and their solid state structure. From a synthetic point of view, 18 molecules of the collection were prepared by the research group for other projects or for other types of experiments and the remaining 5 structures were found in CSD database, in order to extend the study and to have a full collection of all the symmetrical distyrylbenzene substituted with methoxy groups. The synthesis of the structures will be discussed in another section.

The study began with the analysis of PLATON files where it is possible to find the contacts and other geometrical properties. A contact is defined as the situation where the distance between two atoms is less than their Van der Waals radii, they not only include interactions but also geometrical proximity that do not take part in the crystal packing.

It continued with the analysis of outputs of DFT calculations, where are identified the interactions. Not all the interactions for a structure appear in the respective PLATON file, and not all the contacts can be found in the output of DFT calculations.

Usually, the addition of heteroatoms in organic molecules leads to strong intermolecular interactions based on charge gradient and increased the polarization of the molecule, but in this case one of the main intermolecular driving force is between atoms with similar charge. We

became interested in the analysis of CH. . . H interactions because we found them ubiquitous in the DFT calculations of the collection of structures, this kind of intermolecular interaction was found in 15 compounds out of 23.

In the following image (Fig.12) is possible to see the structure (E,E)-1,4-bis(2-(2,4,6-Trimethoxyphenyl)ethenyl)-2,5-dimethoxybenzene opened with Mercury software, where we can notice that most of intermolecular interactions are centred on the methoxy groups in the central benzene ring.

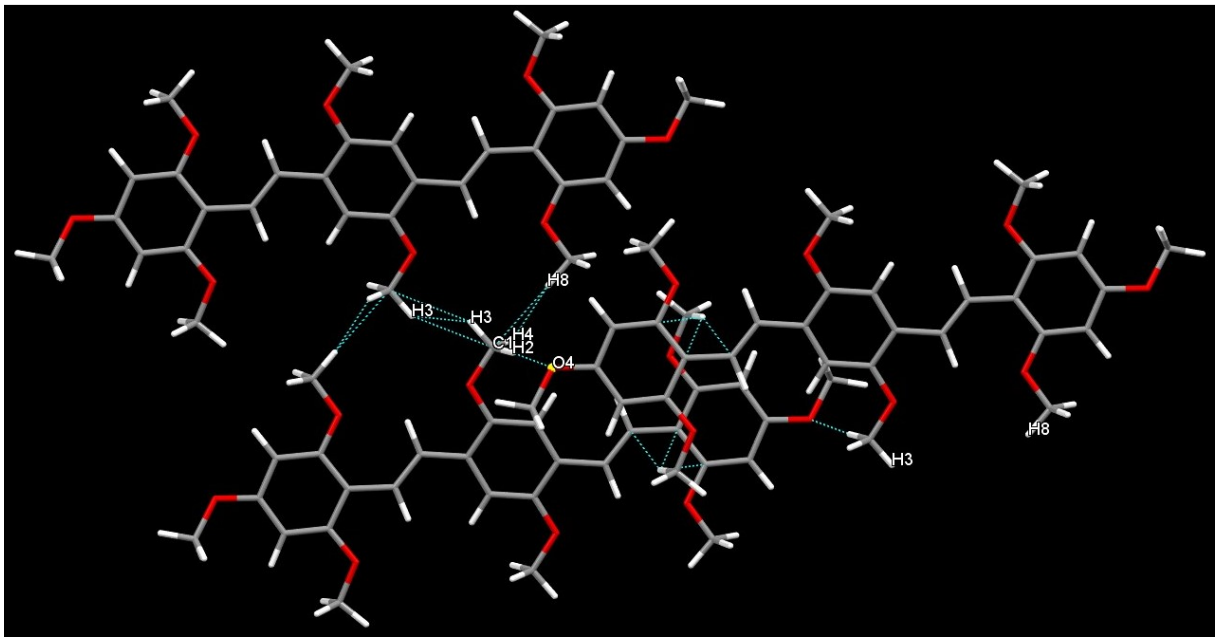

Figure 12: Example of contacts for (E,E)-1,4-bis(2-(2,4,6-Trimethoxyphenyl)ethenyl)-2,5-dimethoxybenzene

The most interesting and strongest interaction in this case is a CH...H intermolecular interaction involving H3 and H3, and the second strongest H4 and H8. Moreover the strongest CH...O intermolecular interaction is weaker than the other intermolecular interactions using the electron density. In the table below (Tab.2) is possible to notice that not only the two strongest interaction involve only hydrogens and no heteroatoms but also that there are a lot of CH...H interactions, that appear to be the main driving force for the crystal packing. Moreover, we identified another type of CH...π intermolecular interacions. We proceed in the same way also for the crystal structure of the molecule (E,E)-1,4-bis(2,3,4- trimethoxystyryl)-2,5-dimethoxybenzene where we found that the two strongest intermolecular driving forces were CH...H interactions.

D	X	Y	X...Y(A°)	Angle	C (pi)	E.d	Laplacian	Bond type	P1/R1	P2/R2
C1	H3	H3	2.1	123		0.00957	0.0266	CH-H	1.03	1.03
C7	H4	H8	2.25			0.00818	0.0267	CH-H	1.00	1.21
C12	H10	Cg1	2.58	8.16	C3	0.00796	0.0242	CH-π		
C12	H16	C8	2.59			0.00780	0.0237	CH-π(6)		
C1	H4	Cg2	2.74	7.78	C13	0.00590	0.0170	CH-π		
C15	H1	C4				0.00569	0.0145			
C1	H2	O4	2.71	121		0.00550	0.0192	CH-O		
C5	H5	H13	2.4			0.00540	0.0161	CH-H	1.00	1.09
C7	H7	C5				0.00536	0.0145			
C12	H10	H1				0.00495	0.0174	CH-H	1.03	1.08
C7	H7	O2				0.00467	0.0178			
C1	H3	O4				0.00439	0.0174			
C15	H11	C7				0.00437	0.0143			
C7	H14	H14				0.00392	0.0118			
C15	H17	O4				0.00390	0.0148			
C7	H14	C11				0.00385	0.0099			
	C13	C2				0.00296	0.0080			
	O4	O4				0.00264	0.0107			
C15	H17	H12				0.00228	0.0068			
C11	H12	O1				0.00176	0.0056			
C6	H9	H9				0.00077	0.0017			

*Table 2: intermolecular interactions for **[246MeO][25MeO]**. In the table the columns **D** represent the labeled atom bonded with one of the atoms involved, the columns **X** and **Y** are the atoms or centroids involved in the interaction; **X...Y** is the distance between the atoms expressed in angstrom, **C(pi)** is the carbon atom reported in DFT calculation instead of the centroid, **E.d** is the electron density of the interaction and **P/R** represent a parameter that describe the curvature of the bond path.*

To better understand how the CH...H interactions worked in the second part of the project, we run non-covalent interaction or NCI calculations in order to analyse one by one every CH...H interaction in the two selected structures. With this type of calculation, it is possible to have a graphical output of the shape of the interaction and to determine where electron density is concentrated on a colour scale. It is also possible to fragment the groups of atoms in order to see their contribution in the interaction.

This type of calculations have been performed before for the interactions of the crystal structure of 2,2'-((1E,1'E)-(2,5-dimethoxy-1,4-phenylene)bis(ethene-2,1-diyl))bis(1,3,5-trimethoxybenzene) and after for the molecule 4,4'-((1E,1'E)-(2,5-dimethoxy-1,4-phenylene)bis(ethene-2,1-diyl))bis(1,2,3-trimethoxybenzene) in order to verify our hypothesis. The image below (Fig. 13) is an example of a NCI calculation's output elaborated with software VMD.

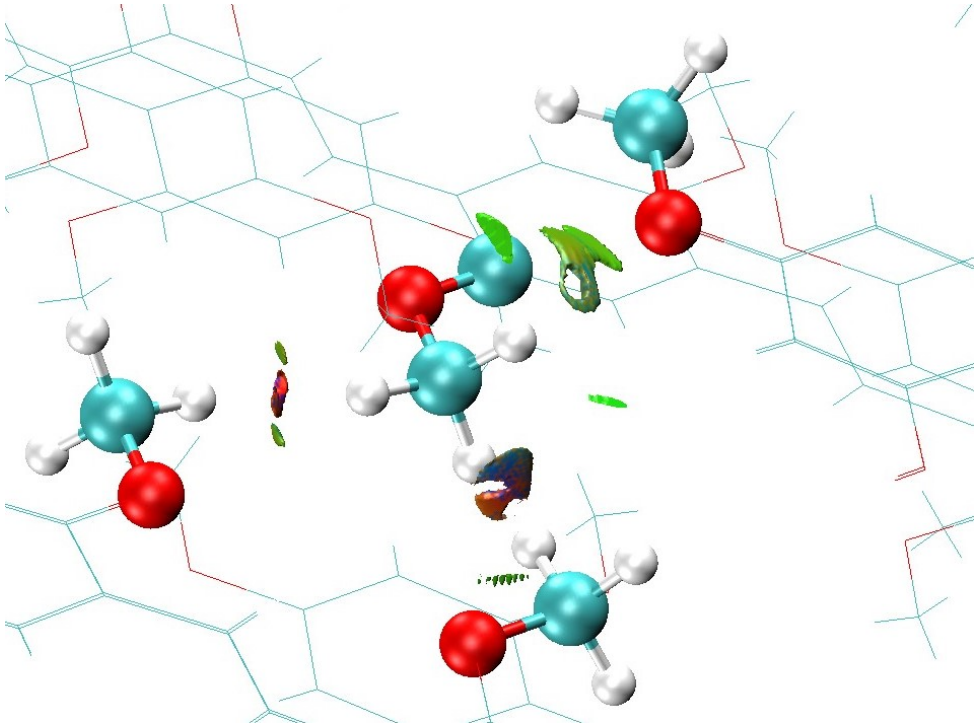

Figure 13: example of NCI calculation that consider the interactions that involve the central methoxy group of [246MeO][25MeO]

We have found three different types of CH...H interactions: the first involves only the two hydrogen atoms cited in the DFT output, it is characterized by a high value of electron density and by a straight bond path; the second type involves a hydrogen that can be interpreted as the donor atom and a methoxy group or part of it that is generally considered as the acceptor group, it is characterized by a low value of electron density and by a large area of interaction; the last type of CH...H involves two methoxy groups, in this case we don't recognize the donor and the acceptor group.

With this project, we don't want to determine if it can be considered as a bonding or non bonding interaction, even if our opinion will be express in the "conclusion" section, but only highlight their apparent importance for crystal packing.

3 Discussion of results

3.1 Collection of structures

The collection of structures is made by 23 crystal structures with the respective .cif files. Part of the collection (18 structures) was synthetized, analysed and characterized with XRD single crystal analysis during previous studies[20], the other part was found in the CSD database. In order to have an easier identification of compounds, they were named using the position of methoxy groups around the external and the central ring as shown in (Fig.14); the molecules are symmetrical with respect to the central ring, so the substitutions on left and right ring are exactly the same and they are arranged in the same way.

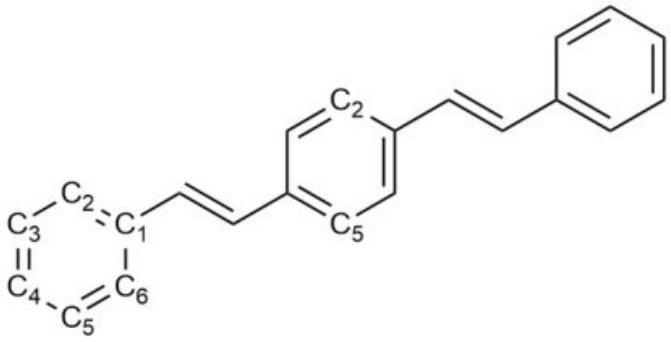

Figure 14: Model used to name the structures based on the position of methoxy groups on the numbered carbon atoms of external and central ring

The structure [246MeO][25MeO] for example bears 3 methoxy groups in the external rings on carbons C2, C4 and C6 and two methoxy groups in the central ring on carbons C2 and C5; if the molecule does not have methoxy groups on the central ring this is indicated with empty brackets "[]".

In the table below (Fig.15) it is possible to see the structures with the name based on the position of methoxy groups and the ID of the structures found in the CSD database in order to have a complete overview of the structures. For all the structures have been analysed the PLATON files and the output of DFT calculations, but for only for structures [246MeO][25MeO] and [234MeO][25MeO] NCI plot calculations were performed.

ID methoxy substitution	ID CSD database	structure
[2MeO][]		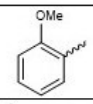
[3MeO][]		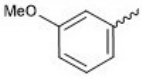
[23MeO][]		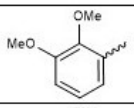
[24MeO][]		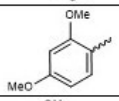
[25MeO][]		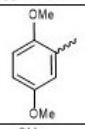
[26MeO][]		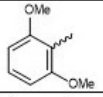
[34MeO][]		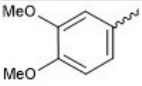
[35MeO][]	REDWUS	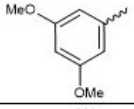
[234MeO][]		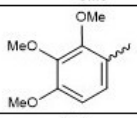
[236MeO][]		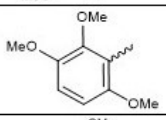
[245MeO][]		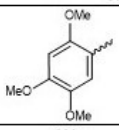
[246MeO][]		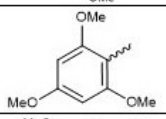
[345MeO][]	JACBIY	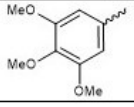

ID methoxy substitution	ID CSD database	structure
[4MeO][25MeO]	QORCEH	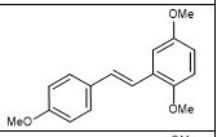
[23MeO][25MeO]		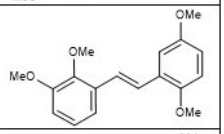
[24MeO][25MeO]		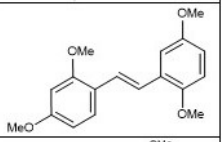
[25MeO][25MeO]		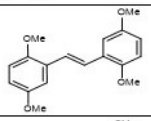
[26MeO][25MeO]		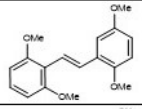
[45MeO][25MeO]		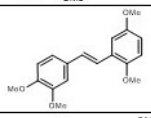
[234MeO][25MeO]		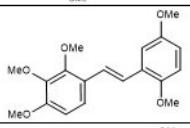
[236MeO][25MeO]		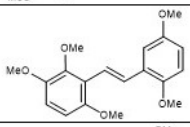
[246MeO][25MeO]	BEZYAH	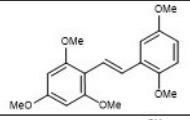
[345MeO][25MeO]	GAKZAU	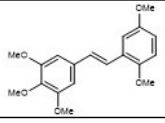

Figure 15: Collection of structures with CCDC code, and disposition of the methyl groups. A

3.2 Analysis of PLATON files

To better understand the crystal packing and the contacts between the molecules in the crystal structures, we analysed the PLATON files of the collection of structures. The PLATON files were directly originated from the .cif files that are the standard output of XRD analysis; the cif files were elaborated with PLATON software to generate a text file.

In the PLATON files all the geometrical properties of the crystal structure are expressed as the list of the centroid in the molecule, the analysis of the crystal geometry, and a list of intramolecular and intermolecular contacts, with some important parameters as the value of distance, angles and the symmetry code of the atoms involved in the contact (Fig. 16).

The label of the atoms is not the same we used to identify the molecules as described in the previous section, but it was arbitrarily given during the XRD analysis. Moreover, in this type of files a contact is identified when the distance between the atoms involved in the contact is less than the sum of their Van der Waals radii and the angle is greater than 90°.

At(I)	[1555.01]	At(J)	[ARU(J)]	D(I-J)	SumRad	Del	Type	X(I)	Y(I)	Z(I)	X(J)	Y(J)	Z(J)	X	X - I...J
O1	....	O2	[ ]	2.6581(18)<<	3.04	-0.38	Intra	0.4036	0.1420	0.2612	0.2608	-0.1055	0.3393		
O1	....	C7	[ ]	2.755(2)<<	3.22	-0.46	Intra	0.4036	0.1420	0.2612	0.3292	0.1770	0.1309	C12	111.11(11)
O1	....	H7	[ ]	2.37<<	2.72	-0.35	Intra	0.4036	0.1420	0.2612	0.3825	0.2997	0.1590		
O1	....	C12	[2645.01]	3.345(2)	3.22	0.13		0.4036	0.1420	0.2612	0.6538	-0.1924	0.2047	C12	160.47(10)
O1	....	H12B	[2645.01]	2.62 <	2.72	-0.10		0.4036	0.1420	0.2612	0.5556	-0.0990	0.1870	C12	166
O2	....	O1	[ ]	2.6581(18)<<	3.04	-0.38	Intra	0.2608	-0.1055	0.3393	0.4036	0.1420	0.2612	C111	176.08(13)
O2	....	C12	[ ]	3.003(2)<<	3.22	-0.22	Intra	0.2608	-0.1055	0.3393	0.3462	0.3076	0.2953	C111	153.96(11)
O2	....	H4	[ ]	2.71 <	2.72	-0.01	Intra	0.2608	-0.1055	0.3393	0.0549	-0.3640	0.2789		
O2	....	H12C	[ ]	2.40<<	2.72	-0.32	Intra	0.2608	-0.1055	0.3393	0.2828	0.2538	0.3359	C111	135
O2	....	H3	[2555.01]	2.70 <	2.72	-0.02		0.2608	-0.1055	0.3393	0.0038	0.1312	0.3392		
O2	....	C11	[4555.01]	3.239(2)	3.22	0.02		0.2608	-0.1055	0.3393	0.5460	0.0383	0.4387	C5	142.52(10)
O6	....	C7	[ ]	2.859(2)<<	3.22	-0.36	Intra	0.1098	-0.1111	0.0772	0.3292	0.1770	0.1309	C16	176.54(13)
O6	....	C8	[ ]	2.834(2)<<	3.22	-0.39	Intra	0.1098	-0.1111	0.0772	0.3422	0.1899	0.0677	C16	151.18(12)
O6	....	H3	[ ]	2.66 <	2.72	-0.06	Intra	0.1098	-0.1111	0.0772	-0.0038	-0.3688	0.1608		
O6	....	H8	[ ]	2.15<<	2.72	-0.57	Intra	0.1098	-0.1111	0.0772	0.2897	0.0696	0.0382	C2	106
														C16	132
O6	....	H16B	[3555.01]	2.86	2.72	0.14		0.1098	-0.1111	0.0772	0.0092	0.2309	0.0024	C2	128
														C16	100
C1	....	C4	[ ]	2.814(2)<<	3.40	-0.59	Intra	0.2537	0.0221	0.1682	0.1118	-0.2569	0.2483	C7	175.69(12)
C1	....	C12	[ ]	3.311(3) <	3.40	-0.09	Intra	0.2537	0.0221	0.1682	0.3462	0.3076	0.2953	C2	144.16(11)
C1	....	H8	[ ]	2.76 <	2.90	-0.14	Intra	0.2537	0.0221	0.1682	0.2897	0.0696	0.0382	C6	161
C1	....	H4	[2555.01]	3.01	2.90	0.11		0.2537	0.0221	0.1682	-0.0549	0.1360	0.2211	C7	116
C1	....	H12B	[2645.01]	2.70<<	2.90	-0.20		0.2537	0.0221	0.1682	0.5556	-0.0990	0.1870	C2	117
C2	....	C5	[ ]	2.782(2)<<	3.40	-0.62	Intra	0.1456	-0.1216	0.1425	0.2172	-0.1207	0.2749	O6	176.95(14)
C2	....	C8	[ ]	3.137(3)<<	3.40	-0.26	Intra	0.1456	-0.1216	0.1425	0.3422	0.1899	0.0677	C3	171.57(12)
C2	....	H8	[ ]	2.85 <	2.90	-0.05	Intra	0.1456	-0.1216	0.1425	0.2897	0.0696	0.0382	C3	164
C2	....	H16A	[ ]	2.67<<	2.90	-0.23	Intra	0.1456	-0.1216	0.1425	0.0623	-0.4067	0.0567	C1	151
C2	....	H16C	[ ]	2.67<<	2.90	-0.23	Intra	0.1456	-0.1216	0.1425	-0.1034	-0.2546	0.0713	C1	156
C2	....	H4	[2555.01]	2.98	2.90	0.08		0.1456	-0.1216	0.1425	-0.0549	0.1360	0.2211	O6	114
C3	....	C6	[ ]	2.748(2)<<	3.40	-0.65	Intra	0.0779	-0.2579	0.1819	0.2889	0.0164	0.2349	H3	179
C3	....	C16	[ ]	2.786(3)<<	3.40	-0.61	Intra	0.0779	-0.2579	0.1819	0.0091	-0.2593	0.0491	C4	179.82(14)
C3	....	H16A	[ ]	2.78 <	2.90	-0.12	Intra	0.0779	-0.2579	0.1819	0.0623	-0.4067	0.0567	C4	158
C3	....	H16C	[ ]	2.69<<	2.90	-0.21	Intra	0.0779	-0.2579	0.1819	-0.1034	-0.2546	0.0713	C4	157

Figure 16: Extract of PLATON file of molecule [236MeO][]

The image above (Fig.17) is only a part of the list of contacts, in the image there are a lot of different type of intermolecular contacts can be identified because of the blank space in the column "Type", as contacts between oxygen and hydrogen, between hydrogen and carbon or between two hydrogen as is reported in the end of the contact list of the PLATON file.

Focusing our attention on one intermolecular contact as the one between O1 and H12B we

can identify the distance between the atoms (2.62 $\AA$), that is less than the sum of their Van der Waals radii (2.72 $\AA$) and the angle between the atoms (166°). The contact can be visualized opening the cif file with the software "Mercury" (Fig.17)

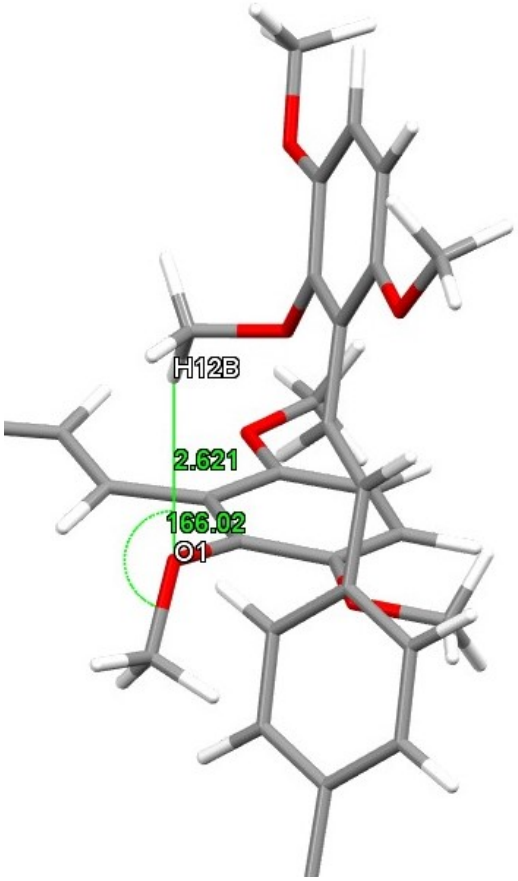

Figure 17: Contact H12B-O1 visualized with mercury

Moreover, this kind of file does not only characterize contacts between two specific atoms, but also between two centroids of a benzene ring (π-π) or between a hydrogen and the centroid of a benzene ring (CH-π)(Fig.18). Contacts π-π have been defined as the situation where the distance between centroids is less than 4.2 $\AA$ and the β angle is less than 30 degrees. Contacts CH-π have been defined as the situation where the distance between the hydrogen and the centroid is less than 3.0 $\AA$ and the γ angle, the angle between Cg-H vector and centroid's normal, is less than 30 degrees.

In the image below (Fig.18) there is an example of the two type of contacts cited before for the crystal structure of the molecule [236MeO][], in this case Cg1 correspond with the centroid of the external ring and Cg2 with the one of the central ring, even if the parameters are different the important variables are the distances and the specific angles.

Cg(I)	Res(I)	Cg(J)	[ARU(J)]	Cg-Cg	Transformed J-Plane P, Q, R, S		Alpha	Beta	Gamma	CgI_Perp	CgJ_Perp
Cg1	[1] ->	Cg1	[2555.01]	4.9385(15)	-0.7565-0.6424 0.1224	0.5609	79.94(8)	14.5	84.2	0.5012(7)	4.7815(7)
Cg1	[1] ->	Cg2	[1545.01]	5.8209(17)	0.8561-0.3471 0.3829	4.8033	34.54(8)	40.9	72.4	1.7592(7)	4.3973(7)
Cg1	[1] ->	Cg2	[3655.01]	5.8209(17)	-0.8561 0.3471-0.3829	-4.8033	34.54(8)	40.9	72.4	1.7592(7)	4.3973(7)
			Min or Max	4.938			34.5	14.5	84.2	-1.759	-4.781

[2555] = -X,1/2+Y,1/2-Z
[1545] = X,-1+Y,Z
[3655] = 1-X,-Y,-Z

X--H(I)	Res(I)	Cg(J)	[ARU(J)]	H..Cg	Transformed J-Plane P, Q, R, S		H-Perp	Gamma	X-H..Cg	X..Cg	X-H,Pi
C4 -H4	[1] ->	Cg1	[2545.01]	2.67	-0.7565-0.6424 0.1224	4.8412	-2.67	1.45	147	3.635(2)	59
C111 -H11B	[1] ->	Cg2	[2645.01]	2.94	-0.8561-0.3471-0.3829	-7.0906	2.88	11.80	139	3.829(2)	42
C111 -H11B	[1] ->	Cg2	[4555.01]	2.94	0.8561 0.3471 0.3829	7.0906	-2.88	11.80	139	3.829(2)	42
			Min or Max	2.670			-2.878	1.5	147.00	3.635	59.00

[2545] = -X,-1/2+Y,1/2-Z
[2645] = 1-X,-1/2+Y,1/2-Z
[4555] = X,1/2-Y,1/2+Z

Figure 18: Example of π-π and CH-π in the PLATON file of molecule [236MeO][]

For the considered crystal structure there are no π-π contacts following the rules cited before, but there are two CH-π contacts. Using Mercury software is possible to visualize them (Fig.19).

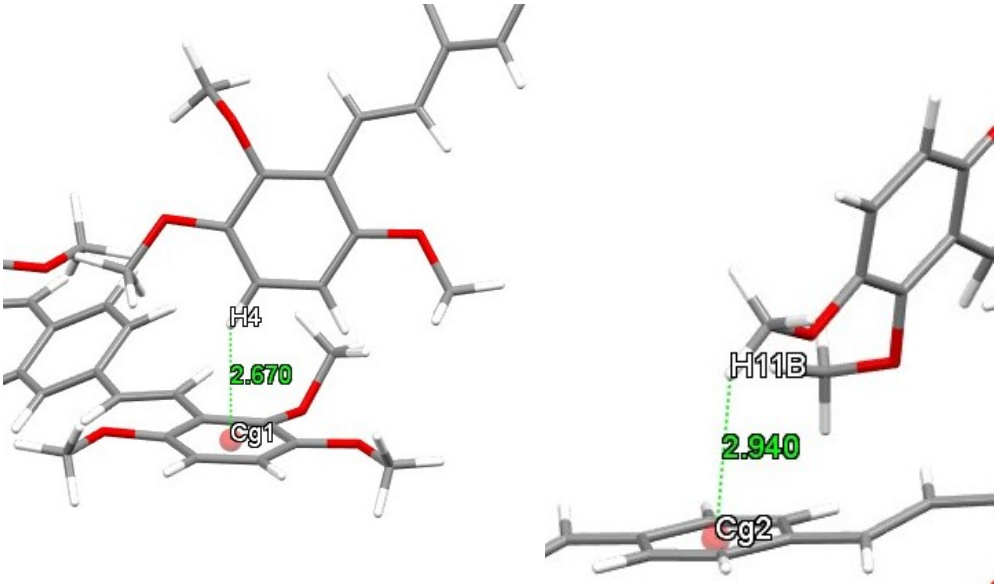

Figure 19: Example of CH-π contact visualized with mercury

This kind of analysis was carried on for all the collection of compounds in order to identify the main types of contacts in the crystal structure, moreover these data were combined with the output of DFT calculations in order to observe the correspondence between contacts and interactions. As was expressed before the contact is based on geometrical parameters, however the interaction is based on the presence of a critical point between the atoms involved, so not all the interactions correspond with a contact and not all the contacts correspond to an interaction.

3.3 Analysis of DFT calculations' output

The calculations were performed on the full collection of structures.

DFT calculations are central to our project in order to find the intermolecular interactions in the crystal structures. In the output files there are a lot of important parameters as the value of electron density that describe the strength of the interaction, the laplacian useful to have an idea of the shape of interactions and other variables as the eigenvalues, the ellipticity and "p" useful for the characterization of C-H...H interactions in the next section.

The labels used for the atoms in the calculation's output are not the same used in PLATON, but were manually modified in order to have an easier interpretation of the results. In the output there are not only the intermolecular interactions, but also intramolecular interactions and the covalent bonds; in order to select only intermolecular interactions, only critical points with values of electron density under 0.013 have been considered.

The DFT calculation output is initially a .cro file but to better read it, it was converted into .csv file and exported in Excel software in order to select only the intermolecular interactions.

From the initial Excel file were selected only the intermolecular and they were used to build a table that summarize the properties of the interactions with the correspondent geometrical parameters from the analysis of PLATON files. The table below (Tab.3) is a good example of what have been done for the full collection of structures and it is referred to the intermolecular interactions of the structure [45MeO][25MeO].

D	X	Y	X....Y (A°)	Angle	C (pi)	E.d	laplacian	Bond type
C12	H15	O3	2.35	144		0.0113	0.0406	CH-O
C5	H7	O2	2.41	130		0.0097	0.0344	CH-O
C6	H4	Cg1	2.73	14.2	C3	0.0078	0.0224	CH-π
C12	H11	Cg2	2.66	7.41	C8	0.0067	0.0207	CH-π
C5	H7	O1	2.67	120		0.0063	0.0245	CH-O
C5	H3	Cg1	2.81	9.99	C13	0.0062	0.0188	CH-π
C12	H13	C2	2.9			0.0059	0.0149	CH-π(6)
C6	H6	C7	2.79			0.0059	0.0155	CH-π(6)
C12	H15	H14	2.25	114		0.0059	0.0175	CH-H
C5	H5	O2	2.71	103		0.0057	0.0195	CH-O
C12	H13	H4				0.0053	0.0178	
C12	H11	H6				0.0052	0.0178	
C5	H3	H1				0.0048	0.0153	
C13	H12	H8				0.0046	0.0133	
C1	H1	C3				0.0045	0.0131	
C11	H10	H8				0.0041	0.0119	
C13		C2				0.0037	0.0096	
C7		C7				0.0032	0.0095	
C7		C7				0.0032	0.0096	
C5	H3	H12				0.0028	0.0103	
C11	H10	H14				0.0012	0.0041	

*Table 3:Intermolecular interactions for structure **[45MeO][25MeO]***

The interactions were categorized using the atoms involved, three types of interactions were identifies using that method: C-H...O interactions, C-H...H interactions and C-H...C. The last type of interaction in some cases can be interpreted as a C-H...π interaction and so can be found correspondence in the PLATON file of molecule [45MeO][25MeO], but in other cases the hydrogen interacts with a centroid that is not recognized by the PLATON file (Fig.21).

These tables were built in order to have an overview of the driving forces and to try to understand how the different disposition and number of methoxy groups can influence the crystal

packing. To complete this analysis was created a table that list for every molecule the number of C-H...O, C-H...H and C-H...π interactions.

In the table below (Tab.4), there are two different columns for C-H...π interactions, in the left one are listed all the interactions where the π system is based on benzene ring and in the right column are listed the interactions where the π system is not based on benzene ring and the distance between the hydrogen and the centroid is less than 3.0 A. In the other columns are listed the C-H...O and C-H...H interactions that were found in PLATON file and in DFT calculations' output.

Molecule	Number of CH-O* interactions	Number of CH-π*° interactions	Number of CH- π^ interactions	Number of CH-H* interactions
[236MeO][]	1	3	2	1
[26MeO][]	2	2	4	1
[236MeO][25MeO]	1	1	1	\
[345MeO][]	3	2	1	\
[26MeO][25MeO]	1	\	1	\
[24MeO][]	1	1	2	2
[234MeO][]	1	3	1	1
[246MeO][25MeO]	1	2	1	3
[234MeO][25MeO]	4	\	1	2
[4MeO][25MeO]	5	5	1	3
[45MeO][25MeO]	4	3	2	1
[3MeO][]	2	1	1	\
[35MeO][]	2	2	2	1
[34MeO][]	2	1	1	1
[345MeO][25MeO]	3	1	\	1
[2MeO][]	1	5	\	\
[25MeO][25MeO]	6	3	\	2
[25MeO][]	1	2	3	\
[24MeO][25MeO]	2	2	2	\
[246MeO][]	1	2	3	2
[245MeO][]	3	3	1	\
[23MeO][25MeO]	4	2	\	1
[23MeO][]	2	4	1	3

*For all the interactions was found the correspondent contact on PLATON file

^ The list includes only π systems different from benzene with a distance < 3 A°

°The list includes only π system based on benzene

Table 4: List of intermolecular interactions for the collection of structures

It is possible to notice that the most frequent intermolecular interaction is the C-H...O as was expected from a collection of molecules with a variable number and distribution of methoxy groups, but something really unexpected was the ubiquitous presence of C-H...H interactions that were found in 17 of 23 structures. Moreover, the C-H...H interaction represented in some structures the strongest intermolecular interaction.

To better understand the behaviour of C-H...H interaction was created a table (Fig.23) where were listed all the C-H...H interactions of the 23 structures, including parameters as electron density, distance, angle and p and r factors; "p" is the length of the bond path from the atom to the critical point and the second is the length of the imaginary line that connect directly the atom with the critical point. The curvature of the interaction can be evaluated by using the p/r value.

Using the table below (Tab.5), it was decided to focus the attention on two molecules that showed the highest value of electron density for C-H...H interaction: [246MeO][25MeO] and [235MeO][25MeO]. These two molecules were used to analyse different types of C-H...H interactions using NCI plot calculations.

Molecule	Atom 1	Atom 2	Distance (A°)	Angle	El. density	p1/r1	p2/r2
[246MeO][25MeO]	H3	H3	2.10	123	0.0096	1.03	1.03
[23MeO][]	H9	H6	2.11	149	0.0084	1.01	1.01
[234MeO][25MeO]	H4	H6	2.12	114	0.0084	1.01	1.02
[234MeO][25MeO]	H8	H11	2.08	171	0.0082	1.00	1.00
[246MeO][25MeO]	H4	H8	2.25	97	0.0082	1.00	1.21
[4MeO][25MeO]	H21	H23	2.22	135	0.0078	1.09	1.01
[234MeO][]	H4	H2	2.23	114	0.0077	1.00	1.07
[25MeO][25MeO]	H12	H2	2.31	106	0.0076	1.17	1.03
[25MeO][25MeO]	H11	H3	2.31	133	0.0075	1.03	1.16
[24MeO][]	H12	H8	2.28	112	0.0075	1.04	1.04
[345MeO][25MeO]	H3	H5	2.25	113	0.0073	1.05	1.01
[23MeO][25MeO]	H9	H6	2.16	151	0.0071	1.00	1.00
[35MeO][]	H11	H10	2.26	116	0.0068	1.05	1.01
[246MeO][]	H10	H14	2.41	102	0.0061	1.02	1.21
[26MeO][]	H15	H14	2.29	114	0.0061	1.05	1.00
[4MeO][25MeO]	H12	H10	2.26	137	0.0060	1.00	1.01
[45MeO][25MeO]	H15	H14	2.25	144	0.0059	1.00	1.00
[24MeO][]	H5	H6	2.39	117	0.0057	1.06	1.03
[345MeO][]	H3	H11	2.32	177	0.0056	1.00	1.02
[34MeO][]	H5	H2	2.33	140	0.0056	1.01	1.03
[246MeO][]	H2	H2	2.53	106	0.0054	1.07	1.07
[246MeO][25MeO]	H5	H13	2.40	112	0.0054	1.00	1.09
[236MeO][]	H7	H15	2.52	130	0.0052	1.03	1.13
[23MeO][]	H8	H13	2.39	139	0.0047	1.01	1.01
[23MeO][]	H7	H4	2.49	105	0.0045	1.01	1.11

Table 5: C-H...H interactions of the collections of compounds. The interactions reported were found both in DFT outputs and PLATON files

For the structure [246MeO][25MeO] have been performed different types of DFT calculations considering the crystal structure or the isolated molecule, in relaxed or scf conditions, using different Van der Waals corrections and basis set; all to verify that the method used didn't influence the final results.

Inter\calc (e.d)	bp	d2	d6	d40	novdw	pbe	wc	cri-rx	gas	wfn	wfx
C6-H9...O3	0.020358	0.020751	0.020751	0.020750	0.020751	0.020237	0.020751	0.019725	0.020746	0.019614	0.019614
C5-H5...O2	0.019106	0.019340	0.019340	0.019341	0.019340	0.018944	0.019340	0.019411	0.019166	0.018596	0.018596
C4-H6...H9	0.013209	0.013471	0.013471	0.013472	0.013471	0.013110	0.013471	0.014347	0.013534	0.012555	0.012555
C1-H3...H3	0.009509	0.009567	0.009567	0.009566	0.009567	0.009398	0.009567	0.009499	NA	NA	NA
C7-H4...H8	0.008094	0.008175	0.008175	0.008175	0.008175	0.007999	0.008175	0.008481	NA	NA	NA
C12-H10...C3	0.007798	0.007955	0.007955	0.007955	0.007955	0.007713	0.007955	0.008479	NA	NA	NA
C12-H16...C8	0.007684	0.007797	0.007797	0.007797	0.007797	0.007586	0.007797	0.007746	NA	NA	NA
C1-H4...C13	0.005812	0.005901	0.005901	0.005901	0.005901	0.005735	0.005901	0.006233	NA	NA	NA
C15-H1...C4	0.005649	0.005685	0.005685	0.005685	0.005685	0.005566	0.005685	0.006231	NA	NA	NA
C1-H2...O4	0.005545	0.005499	0.005499	0.005499	0.005499	0.005476	0.005499	0.004500	NA	NA	NA
C5-H5...H13	0.005399	0.005401	0.005401	0.005401	0.005401	0.005327	0.005401	0.005474	NA	NA	NA
C7-H7...C5	0.005323	0.005356	0.005356	0.005356	0.005356	0.005250	0.005356	0.005851	NA	NA	NA
C12-H10...H1	0.004933	0.004952	0.004952	0.004953	0.004952	0.004872	0.004952	0.004621	NA	NA	NA
C7-H7...O2	0.004666	0.004665	0.004665	0.004665	0.004665	0.004610	0.004665	0.005277	NA	NA	NA
C1-H3...O4	0.004392	0.004386	0.004386	0.004386	0.004386	0.004342	0.004386	NA	NA	NA	NA
C15-H11...C7	0.004360	0.004369	0.004369	0.004369	0.004369	0.004317	0.004369	0.004140	NA	NA	NA
C7-H14...H14	0.003914	0.003916	0.003916	0.003916	0.003916	0.003870	0.003916	0.004139	NA	NA	NA
C15-H17...O4	0.003943	0.003898	0.003898	0.003898	0.003898	0.003909	0.003898	NA	NA	NA	NA
C7-H14...C11	0.003840	0.003845	0.003845	0.003845	0.003845	0.003793	0.003845	0.003858	NA	NA	NA
C13...C2	0.002887	0.002958	0.002958	0.002958	0.002958	0.002854	0.002958	0.003092	NA	NA	NA
O4...O4	0.002653	0.002642	0.002642	0.002642	0.002642	0.002648	0.002642	0.003809	NA	NA	NA
C15-H17...H12	0.002302	0.002279	0.002279	0.002279	0.002279	0.002303	0.002279	NA	NA	NA	NA
C11-H12...O1	0.001808	0.001763	0.001763	0.001763	0.001763	0.001813	0.001763	0.001663	NA	NA	NA
C6-H9...H9	0.000773	0.000765	0.000765	0.000765	0.000765	0.000797	0.000765	NA	NA	NA	NA

*Table 6: Intermolecular and intramolecular critical points of molecule **[246MeO][25MeO]** calculated with different methods. The details of the methods are reported in the experimental section*

From the table above (Tab.6) is possible to verify that the number and the entity of critical points is quite stable, clearly for gas phase calculations there are only critical points for intramolecular interactions, so is possible to consider all the critical points as independent of the method used.

3.4 Analysis of NCI plot calculations

NCI calculations are useful to characterize and classify different types of interaction using their shape and the distribution of the electron density, and their output of the calculations was later combined with the results of QTAIM analysis. Initially this analysis was carried on for the structure based on molecule [246MeO][25MeO] and in order to confirm our hypothesis the same thing was done also for the structure [234MeO][25MeO].

In the table 7, are reported all the information from DFT output useful to complete the NCI analysis for the C-H...H interactions of the crystal structure of molecule [246MeO][25MeO].

D	X	Y	X...Y(A°)	Angle	C (pi)	E.d	Laplacian	Bond type	P1/R1	P2/R2
C1	H3	H3	2.1	123		0.00957	0.0266	CH-H	1.03	1.03
C7	H4	H8	2.25			0.00818	0.0267	CH-H	1.00	1.21
C12	H10	Cg1	2.58	8.16	C3	0.00796	0.0242	CH-π		
C12	H16	C8	2.59			0.00780	0.0237	CH-π(6)		
C1	H4	Cg2	2.74	7.78	C13	0.00590	0.0170	CH-π		
C15	H1	C4				0.00569	0.0145			
C1	H2	O4	2.71	121		0.00550	0.0192	CH-O		
C5	H5	H13	2.4			0.00540	0.0161	CH-H	1.00	1.09
C7	H7	C5				0.00536	0.0145			
C12	H10	H1				0.00495	0.0174	CH-H	1.03	1.08
C7	H7	O2				0.00467	0.0178			
C1	H3	O4				0.00439	0.0174			
C15	H11	C7				0.00437	0.0143			
C7	H14	H14				0.00392	0.0118			
C15	H17	O4				0.00390	0.0148			
C7	H14	C11				0.00385	0.0099			
	C13	C2				0.00296	0.0080			
	O4	O4				0.00264	0.0107			
C15	H17	H12				0.00228	0.0068			
C11	H12	O1				0.00176	0.0056			
C6	H9	H9				0.00077	0.0017			

*Table 7: Intermolecular interactions for **[246MeO][25MeO]**, with important parameters for the analysis of NCI plot calculations.*

From the table above, it is possible to see that most of intermolecular interactions involved the methoxy group on the central ring, for this reason the first NCI plot (Fig.20) considered the hydrogens of the central methoxy group.

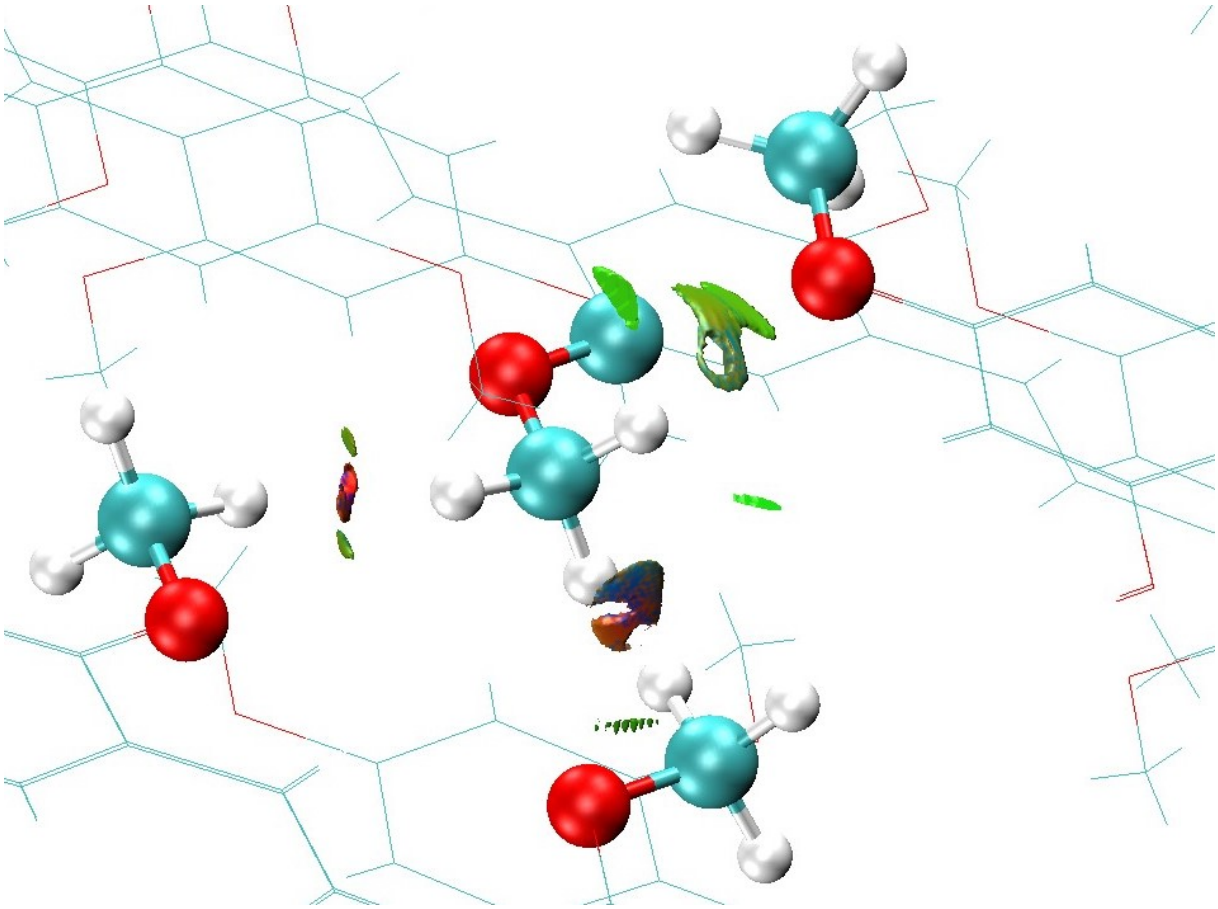

Figure 20: NCI calculation of central methoxy group of [246MeO][25MeO]

So attention was focused on the analysis of single interactions in order to have a better resolution of the shape and to determine the contribution of the atoms to the interaction.

3.4.1 H3...H3 interaction

It is the strongest C-H...H interaction of the collection of compounds, and it is a good example of first type of C-H...H interaction. The NCI calculation (Fig.21) was carried on to analyse the shape of the interaction.

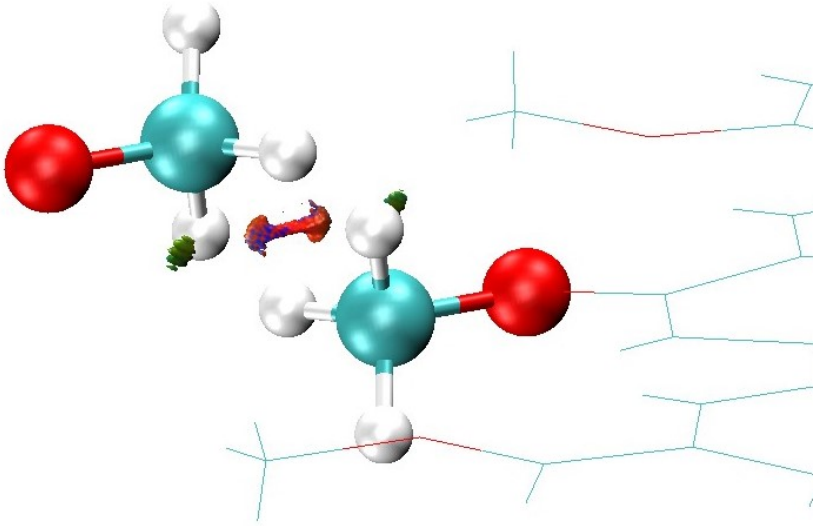

Figure 21: NCI calculation of CH3-H3

The interaction is elongated and appears to be of a vivid red colour that correspond with a negative value of electron density, that means a non-bonding interaction. However, there is also blue region which correspond with a positive value of electron density, so with a bonding interaction.

The molecule was fragmented in order to verify that only the two hydrogens reported in DFT output were involved in the interaction. In the image are also visible two green areas on the left and right side of the main interaction, with electron density nearby zero, that are probably an extremely weak interaction between O1 and H3 (Fig.21). When only the two hydrogens cited in the table in figure 25 are considered, the two green areas disappear.

This interaction is a good example of the first type of C-H...H, even if there are some peculiarities given by the symmetrical groups involved, as the particular shape of the interaction. Generally, the first type of C-H...H interaction is characterized by the direct interaction between the two hydrogens cited in the DFT output. From the analysis of NCI calculations of the other molecules, some similarities with C-H...O interactions were found as the low value of p/r parameter that indicate a straight bond path and the circular interaction's shape.

3.4.2 H8...H4 interaction

For this interaction was used also the imaging output of the QTAIM calculation that shows the bond path (white points) and the position of the critical point (green point), this information was combined with the imaging output of NCI calculation (Fig.22).

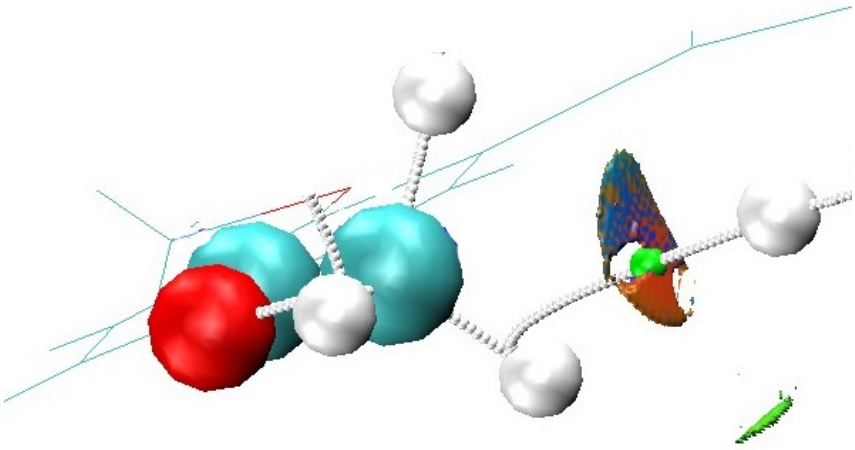

Figure 22: nci calculation of CH8-H4

The interaction is larger than the other described and cover the methyl group, a part of it between H4 and H8 is red, so the electron density in that area is negative, the other part is blue that correspond with a positive value of electron density. Moreover, nearby the methyl group the bond path is quite curved, this is demonstrated also by table 7 where the value of p/r is higher than 1.

The methyl group involved was fragmented in order to see the contribution of every atom to the interaction, this procedure will be described in the subsection characterization of the interaction. From these experiments have been determined that the interaction did not occur between the two hydrogens cited in table 7, but between the hydrogen H8, the donor atom and the entire methyl group, moreover have been determinate that the highest contribution in the acceptor group to the interaction was given by the couple of atoms that involve the carbon atom of the methyl group and the hydrogen H4.

This interaction is a perfect example of the second type of C-H...H interaction because it is involved a hydrogen that is interpreted as the donor atom and a methyl group. From the analysis of other interactions, it was found that this type of interaction can involve also only a part of the methyl-acceptor group this depends on the disposition of the donor atom and of the acceptor.

Moreover, this interaction is characterized by a high value of p/r parameter in the section between the acceptor group and the critical point. In the case described before, the bond path initially point in the direction of the center of the methyl group but in the end it finished on the acceptor hydrogen H4.

3.4.3 H10-H1 interaction

This interaction represent a good example of the third type of C-H...H interaction, for this reason it was analysed using NCI calculations (Fig.23).

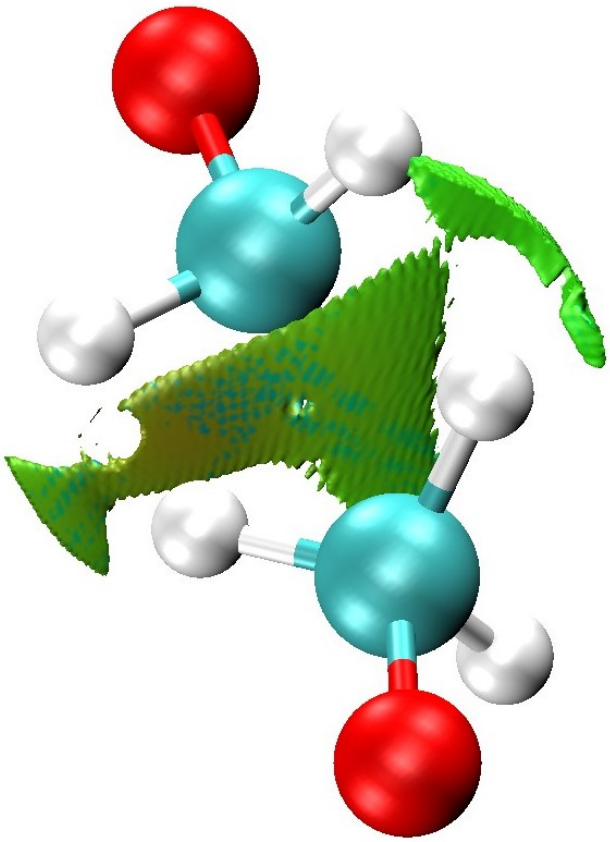

Figure 23: nci calculation of H10-H1

In this case, the interaction is not between only two hydrogens or a hydrogen and a methyl group, but between two methyl groups one facing the other. It is mainly green, so the electron density in the interaction area is nearby zero, there is only a part between the two hydrogen cited in table 7 that is orange, this mean that between the hydrogens there is a non bonding interaction.

Moreover, the groups were fragmented in order to observe the contribution of every atom or fragment of methyl groups to the interaction; but for every couple of fragment, the interaction disappears. We concluded that in this case, the interaction occurred only between the two methyl groups.

The main differences between the three types of C-H...H interactions is the number of atoms involved. This kind of evaluation is possible with the fragmentation of the molecules considered for the NCI calculation. Another possible difference is the different shape of the interactions, the first type of C-H...H interaction is characterized by a small area of interaction however the second and the third types of interactions are characterized by a large area due to the involvement of methyl groups. In the image below (Fig.24-26) are reported the NCI plot of the three types of C-H...H interactions.

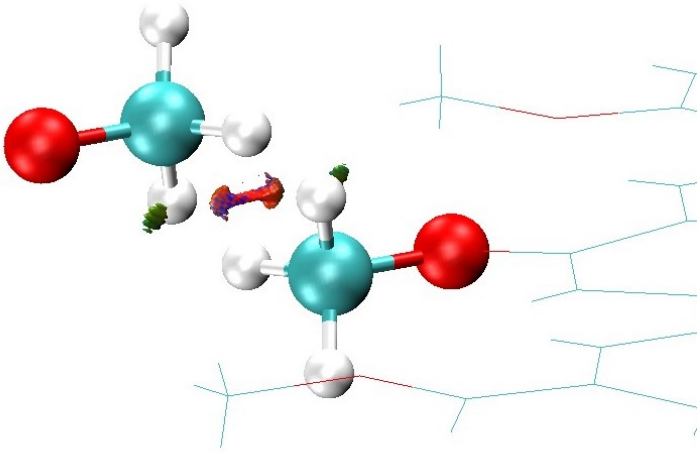

Figure 24: Example of type I of C-H...H interaction

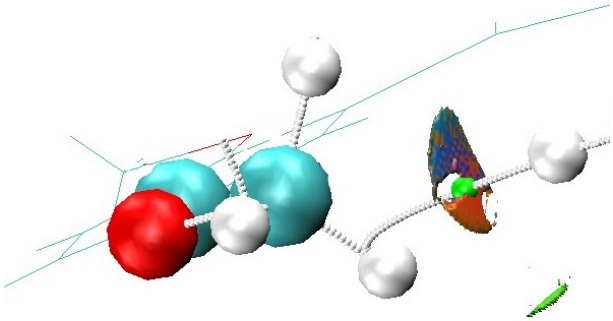

Figure 25: Example of type II of C-H...H interaction

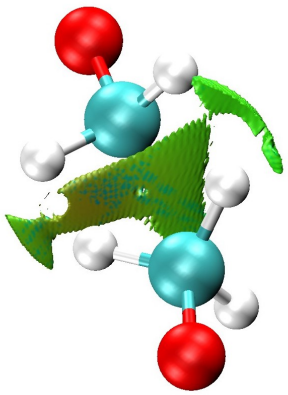

Figure 26: Example of type III of C-H...H interaction

In the end have been realized two tables (Tab.8-9), one for each molecule, where are summarized the C-H...H interactions with the type (I, II or III) according to the parameters expressed before and a short description of their shape and color from NCI analysis.

D	X	A	S. code	Type	Details
C1	H3	H3	-1-x, 1-y, -1-z	I	Small and bilobed shape mainly red with some blue spots
C7	H8	H4	-1-x, 1-y, -1-z	II	Irregular shape mainly blue with a light red area
C5	H5	H13	x, 1+y, z	I	Circular and orange
C12	H10	H1	-x, -3-y, -1-z	III	Triangle-irregular shape, mainly green with a light red area
C7	H14	H14	-x, -2-y, -2-z	I	Rectangular-irregular shape mainly green
C15	H17	H12	-x, -3-y, -2-z	I	Circular-Irregular shape mainly green
C6	H9	H9		II	Irregular shape mainly green

Table 8: summary table of C-H...H interactions of molecule ***[246MeO][25MeO]***

D	X	A	S. code	Type	Details
C2	H4	H6	-x, -y, 1-z	I	Red and circular
C4	H8	H11	x, 1+y, z	I	Red and circular with blue parts
C9	H12	H3	-1-x, 1-y, -z	II	Irregular shape, mainly green with red area in the center. It involves the donor hydrogen and the carbon with two hydrogens of the methyl-acceptor group
C13	H17	H11	x, 1+y, z	II	Irregular shape, mainly green with a faded red area in the center. It involves the donor hydrogen and the carbon with one hydrogen of the methyl-acceptor group
C3	H9	H9	1-x, -y, 1-z	I	Irregular shape mainly green
C6	H13	H16	1+x, -1+y, z	I-II	Irregular shape mainly green with a faded red area . The interaction occurs between the two hydrogens and between the donor hydrogen and part of the acceptor group.
C1	H2	H2	-x, -y, -z	II	Circular and green
C3	H1	H9		III	Irregular shape mainly green
C3	H6	H14		I	Circular shape mainly green
C1	H2	H10		III	Irregular shape mainly green
C9	H15	H2		III	Irregular shape mainly green
C3	H9	H5		II	Irregular shape mainly green
C9	H15	H15		III	Oval shape mainly green

Table 9: summary table of C-H...H interactions of molecule ***[234MeO][25MeO]***

3.5 Characterization of interaction

For the characterization of the C-H...H interactions have been used different computational methods. For the full collection of molecules was analyzed the intermolecular contacts using the PLATON files in order to have an idea of the different types of intermolecular contacts and of their geometrical properties.

Moreover, on the entire set of 23 molecules, DFT calculations were carryed on to identify the intermolecular interactions and to classify them using the atoms involved, the value of electron density, and other values as "p", "r" and "p/r" that describes the curvature of the bond path for an interaction.

Two molecules, [246MeO][25MeO] and [234MeO][25MeO], were selected to perform NCI plot calculations, in order to characterize and classify the C-H...H interactions using the atoms involved in the interaction, the shape of the interaction and the distribution of electron density and parameters from the DFT calculations such as "p/r". The two molecules were selected because they presented many C-H...H interactions and because these in some cases had very high values of electron density.

As example for the characterization of C-H...H interaction is used C7-H8...H4 of molecule [246MeO][25MeO] because it is the interaction with the higher number of nci calculations associated. For every NCI calculation correspond a different fragment, this was done in order to understand the contribution of every atom and portion of molecule to the interaction.

In the beginning have been done the calculation between H8 and the methyl group where compare the hydrogen H4, in this way was obtained the image of the full interaction. The NCI plot has been overlapped with the output of DFT, to see not only the shape of the interaction but also the bond path (white line) and the position of the critical point (green point) (Fig.28), in this way it is possible to undertand better for example the values of curvature for the investigated nteraction.

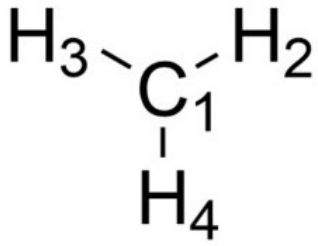

Figure 27: label of the methyl-acceptor group for NCI plot showed below

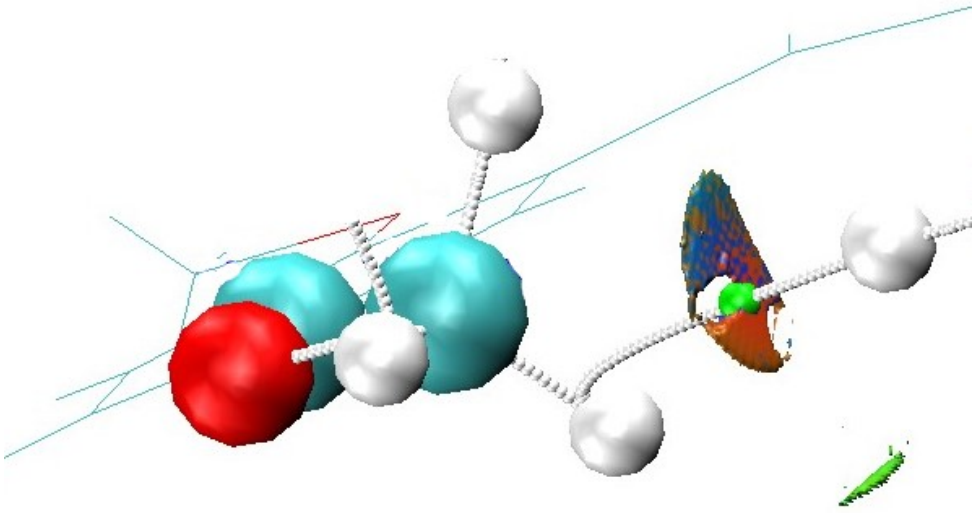

Figure 28: NCI plot of interaction CH8-H4

As it is possible to see from the image above, the interaction is quite large and cover the centre of the methyl group, the colour is mainly blue, this corresponds with a positive value of electron density and so with a bonding interaction, however in the portion of interaction between H4 and H8 it is mainly red, so the associated value of electron density is negative and the type of interaction in that region is non-bonding.

Moreover, the curvature of the bond path was evaluated using the plot, but also the value of p/r from DFT calculation; if is considered the part between the crytical point (green point) and the hydrogen H4, it seems that the bond path initially point to the centre of the methyl group but in the last part it curves in the direction of hydrogen H4.

The methyl group was fragmented to understand the contribution of every part to the interaction, for the correspondent calculations were used the donor hydrogen and different parts of the methyl acceptor group. the output was elaborated to see the shape of the portion of the interaction using VMD software.

Initially, calculations were performed by considering only a couple of hydrogen, the donor and a hydrogen of the methyl group, but nothing was found because every time the output file was empty. For this reason the acceptor group have been fragmented including the central carbon atom and a variable number of hydrogens around it. Initially have been considered only a couple of atoms in the acceptor group, the carbon and one of the hydrogens. The imaging output of these NCI plot calculations was analysed from the same point of view in order to evaluate the contribution of every portion of acceptor group to the interaction.

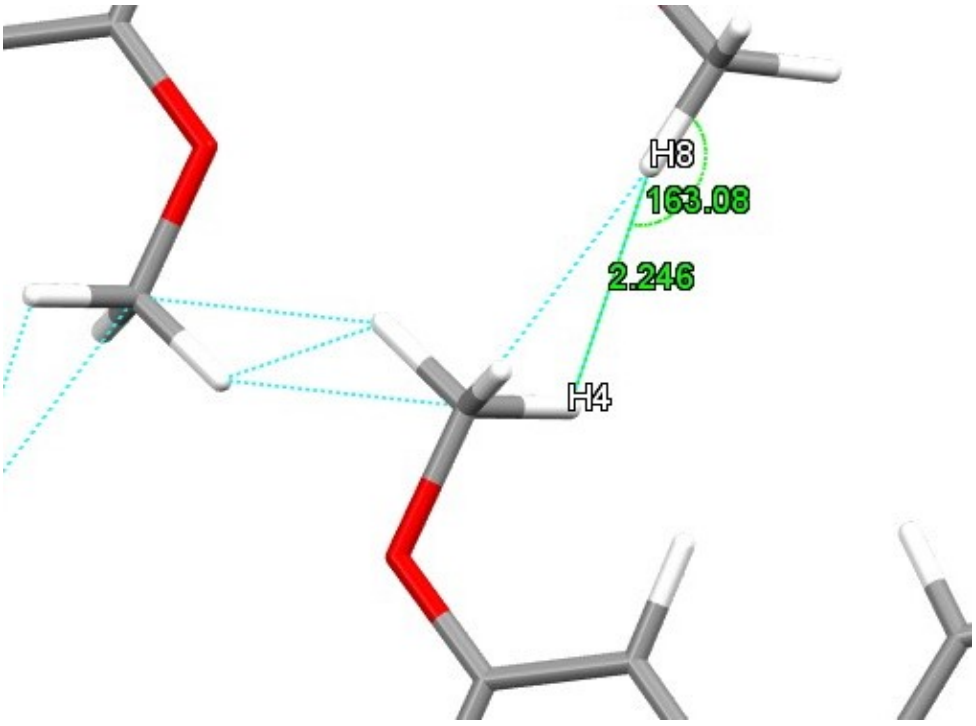

Figure 29: mercury imaging of contact CH8-H4 with geometrical details

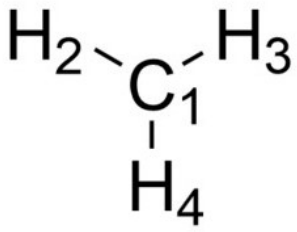

Figure 30: label of the acceptor methyl group in the NCI plot calculations

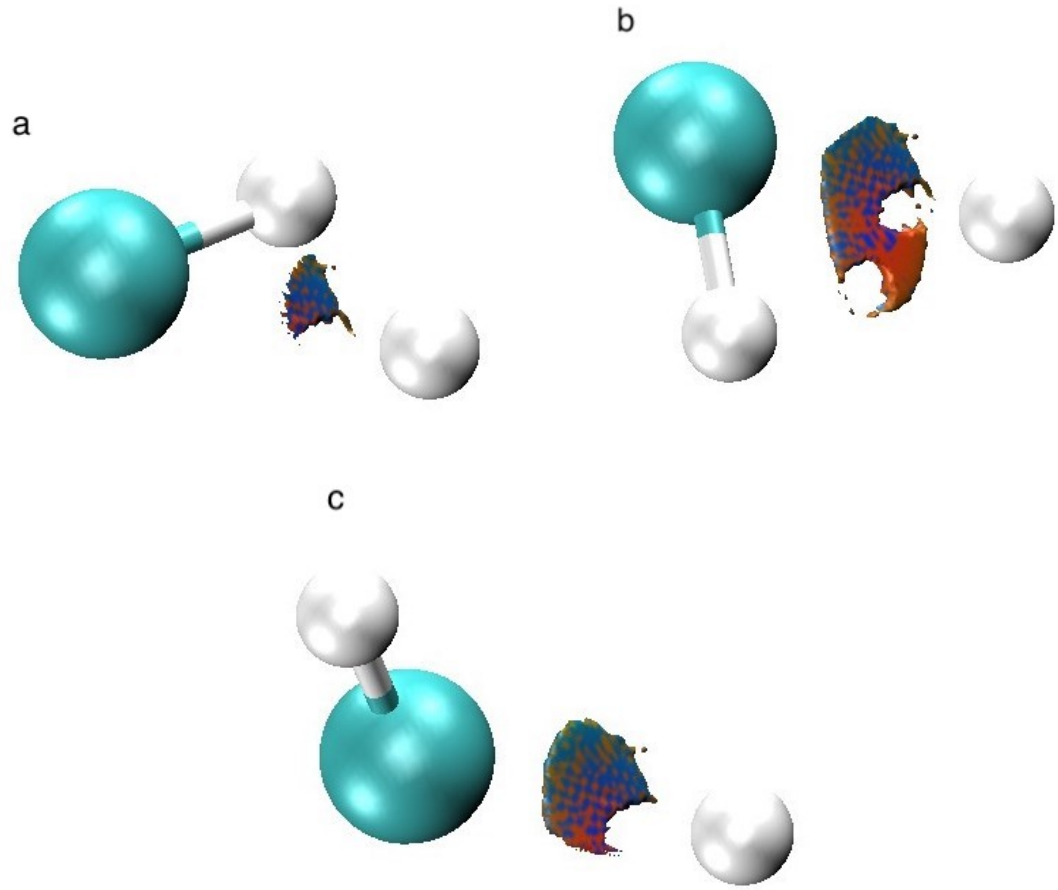

Figure 31: NCI plots of the interaction between H8 and C1-H3 (a), between H8 and C1-H4 (b) and between H8 and between H8 and C1-H2 (c)

From figure 31, can be determined that the fragment that contribute the most to the interaction is C1-H4 (b), where C1 is the carbon of the methyl group and H4 is the hydrogen cited in the DFT output, in this case the interaction has a red part and a blue part. The calculations done on the other fragments are indicative of the important role of the carbon C1 in the interaction, indeed it is everytime present in the NCI calculations.

Moreover, we performed calculations considering the carbon and two hydrogens of the methyl-acceptor group as shown in figure 33.

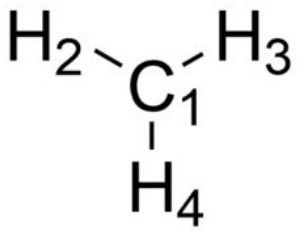

Figure 32: label of the acceptor methyl group in the NCI plot calculations

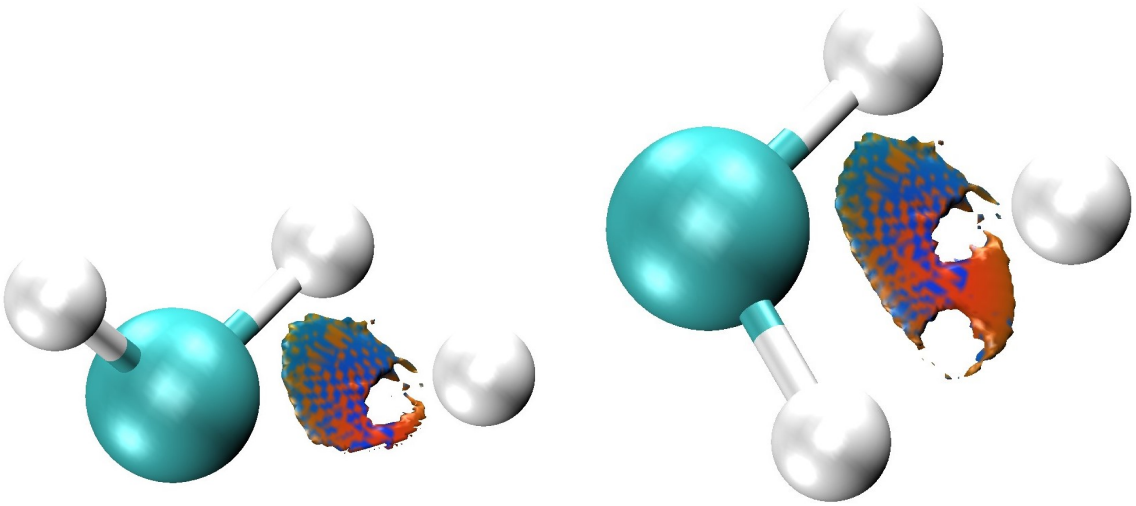

Figure 33: NCI plots of the interaction between H8 and H2-C1-H3 (left), between H8 and H3-C1-H4 (right)

From these calculation is possible to confirm the importance of the carbon atom for the interaction and the great contribution of hydrogen H4 in particular. Most probably, the interaction between the hydrogen H8 and the acceptor group, occur between the donor and the C-H bond between C1-H4.

Other NCI plot calculations have been performed to verify the contribution of the oxygen atom to the interaction but nothing interested was found.

So in the end using the classification described in the previous section, it is possible to classify the interaction in the category of second type of C-H...H interaction, thanks to the evaliuation of the atoms involved and of the shape of the NCI plot.

4 Conclusions

Organic crystal structures such as DSBs have been studied for decades for their important role in hi-tech useful as semiconductor, photoemitter materials or sensors. For this reason, their solid state chemistry is really important in order to understand their behaviour and their properties. To this aim, it is central to study the crystal packing, and in particular the intermolecular interactions. Some of them have been investigated for really long time as C-H...O interaction or C-H...π, but other as C-H...H interactions are still controversial in the scientific community.

During the internship at the Structural Chemistry Group of the University of Antwerp, the research group have started to shed light on the intermolecular interactions that occurs in crystal structures based on distyrilbenzene compounds. Thanks to this, a new type of intermolecular interaction have been found and were made some steps to characterize it.

The aim of this thesis work was to investigate the intermolecular interactions that occur in the crystal structures of a class of compounds (DSBs) in particular C-H...H interactions, and to characterize it using different computational experiments. By analysing in detail the C-H...H intermolecular interactions of the full collection of compounds, it could be possible to understand unexplained phenomena as self-assembly mechanism.

The first part of my project was focused on the analysis of the PLATON files of 23 crystal structures based on methoxy substituted distyrilbenzene molecules. The analysis was important in order to have an idea of the intermolecular contacts in the crystal structures. Moreover, it was found that none of the crystal structure had a π-π contact but were found other type of contacts as C-H...π or C-H...O or C-H...H.

The geometrical data of intermolecular contacts helped us to better understand the correlation between contacts and interactions that comes out in qtaim calculations and helped us to build the table useful to understand the qtaim output.

In the second part of the project, the aim was to explore the output of QTAIM calculations of the collection of structures. For every structure was built a table that show the intermolecular interaction classified using parameters as electron density, laplacian, ellipticity, and the nature

of the atoms involved, moreover were used geometrical data from PLATON files to complete this kind of table.

In the end 4 different types of intermolecular interactions have been found: C-H...O, C-H...π based on benzene ring, C-H...π not based on benzene ring and C-H...H. The last type of interaction was found ubiquitous in the collection of structures, and it is still a very unexplored and controversial driving force. For this reason, we decided to investigate specifically the C-H...H interactions.

In the last part of the project were selected two structures, [246MeO][25MeO] and [325MeO][25MeO] because they showed the strongest and highest number of C-H...H. They were analysed doing NCI calculation for every C-H...H interaction. This kind of calculation gives an imaging output of the shape and dimension of the interaction, with a colour scale that describe the strength of the electron density in the area of the interaction. In the end were identified three different types of C-H...H interaction.

The first one involves only the two hydrogen cited in the qtaim output, it is characterized by a circular shape and has properties similar to the C-H...O interactions. It is often the strongest type of C-H...H interaction.

The second type of C-H...H interaction involves a hydrogen that is interpreted as the donor atom and full or a part of a methyl group that is interpreted as the acceptor group. It is characterized by a large area of interaction and by a curved bond path nearby the acceptor group. Moreover, the molecules involved were fragmented in order to understand the contribution of every part in the interaction.

From the NCI plot calculations done on fragments of the acceptor group it was found that if were included in the computational experiments only the two hydrogens cited in DFT output, the interaction's plot disappears, however if the calculations included the donor hydrogen and part of the acceptor group as the carbon and one hydrogen was possible to identify a portion of interaction. The same thing have been noticed for the third type of C-H...H interaction.

The last type of interaction involves two methyl groups one in front of the other, in this case none of the groups have the role of donor or acceptor. It is characterized by a large area of interaction, and by a very weak electron density. Also for this kind of interaction was realized a lot

of calculations including different portion of methyl groups in order to check their contribution to the interaction.

The C-H...H interactions are still a very controversial and unexplored subject, there are opposite position in the scientific community. For one part, these kinds of interactions can be classified as bonding forces, and this position is proven with DFT calculations and degradation computational experiments focused on the evaluation of degradation energies. However, for the other part the presence of a critical point is not enough to prove the existence of a bonding interaction and in this way the QTAIM theory does not explain everything.

In our opinion, even if we agree with the position that say that the presence of a critical point is not enough to determine the presence of a bonding interaction, this was proved also with the analysis of PLATON files where have bee found that not all the contacts matched with interactions and not all the interactions correspond to a contact, this is probably caused because a contact is defined by geometrical parameters, however an interaction is identified by critical point based on electron density and on other quantum-chemical parameters.

In the end we think that because of the numerous presence of C-H...H intermolecular interactions in the collection of structures, and for the similarities with the C-H...O interactions it is a fundamental driving force for the crystal packing and it could be important to explain the self-assembly mechanism or to get a better understanding of the physical-chemical properties of the crystal structures.

5 Experimental section

5.1 Methods

The calculations were performed using quantum expresso for the collection of compounds. The details of the calculations are resumed in table 10; to obtain the QTAIM output of the crystal structures was used the method D40 (Tab.10). On structures [246MeO][25MeO] were performed other calculations to verify that the method used did not affect the final results the details are described in table 10.

On structures [246MeO][25MeO] and [345MeO][25MeO] were done NCI calculations using a gradient of colour scale between -1 and 1 and a value of increments of 0.04 Bohr in each direction. In the colour code, red colour correspond with a positive value of reduced electron density that correspond with a negative value of electron density, however blue colour correspond with a negative value of reduced electron density, and so with a positive value of electron density and green colour correspond with a negative or positive value of electron density closed to zero.

5.2 Computations

Different types of computational have been performed in order to analyse different parameters of interactions as the electron density or the curvature of the bond path or the shape and the distribution of electron density.

The first computational done have been DFT calculation, all the details of this experiment are described in table 10; one of the experiments has been performed on the full collection of compounds D40, all the other calculations were performed only on [246MeO][25MeO] to verify that the type of experiment did not influence the number and the strength of critical points.

The details of the VdW corrections[21][22][23] and of the functional[24][25][26] are described in the references.

Label	Calculation	Structure	DFT Program	Van der Waals correction	Functional	Basis set	Energy cut off (wfc)	Energy cut off (rho)	AIM program
bp	SCF	Crystal	QE	DFT-D3(0 damping)	BP	\	65 Ry	1300 Ry	Critic2
d2	SCF	Crystal	QE	DFT-D2	WC	\	65 Ry	1300 Ry	Critic2
d6	SCF	Crystal	QE	DFT-D3 (BJ damping)	WC	\	65 Ry	1300 Ry	Critic2
d40	SCF	Crystal	QE	DFT-D3(0 damping)	WC	\	65 Ry	2600 Ry	Critic2
novdw	SCF	Crystal	QE	\	WC	\	65 Ry	1300 Ry	Critic2
pbe	SCF	Crystal	QE	DFT-D3(0 damping)	PBE	\	65 Ry	1300 Ry	Critic2
wc	SCF	Crystal	QE	DFT-D3(0 damping)	WC	\	65 Ry	1300 Ry	Critic2
rel	Relax	Crystal	QE	DFT-D3(0 damping)	WC	\	65 Ry	1300 Ry	Critic2
gas	SCF	Molecule-in-supercell	QE	DFT-D3(0 damping)	WC	\	65 Ry	1300 Ry	Critic2
wfn	Relax	Gas	Gaussian09	\	B3LYP	6-311++G**	\	\	Critic2/AIM2000
wfx	Relax	Gas	Gaussian09	\	B3LYP	6-311++G**	\	\	Critic2

Table 10: DFT calculations' settings

To perform the calculation D40 was submitted a ".slurm" file (Fig.34) where is described the procedure that the super computer has to follow in order to perform the calculation. The slurm file change according to the computational experiment to perform.

The ".slurm" file contain different sections that describe for example the limit of time for the calculation, the name of it and the folder that will be created to place the output; the name of the input and output files and other settings that describe the procedure that the supercomputer has to follow in order to perform the calculations, this part change according to the type of computational experiments and in the last part is described were to upload all the input files for the calculation and the part of the supercomputer to use.

```
#SBATCH --ntasks 28 --nodes 1 --cpus-per-task 1
#SBATCH --time 4:00:00
#SBATCH --job-name 195norm-cri
#SBATCH --output /scratch/antwerpen/208/vsc20851/qe/stdout/stdout.%j.%x
#SBATCH --error /scratch/antwerpen/208/vsc20851/qe/stderr/stderr.%j.%x
#SBATCH --mail-type=all
#SBATCH --mail-user=filippo.vacchi@student.uantwerpen.be

mkdir -p /scratch/antwerpen/208/vsc20851/qe/195norm-cri
directory="/scratch/antwerpen/208/vsc20851/qe/195norm-cri"

cd ${SLURM_SUBMIT_DIR}

# copy_commands
cp 195norm-cri.scf.in $directory
cd $directory
cat > 195norm-cri-ae.pp.in <<-EOD
&inputpp
    prefix  = '195norm-cri'
    outdir = './'
    filplot = '195norm-cri-ae'
    plot_num= 21
/
&plot
nfile = 1
iflag = 3
output_format = 6
fileout = '195norm-cri-ae.cube'
/
EOD
cat > 195norm-cri.cri <<- EOD
CRYSTAL 195norm-cri-ae.cube
LOAD 195norm-cri-ae.cube id rhoae smoothrho
REFERENCE rhoae
AUTO EPSDEGEN 1E-7 SEED PAIR SEED WS DISCARD "\$rhoae < 9e-5"
CPREPORT 195norm-cri.vmd graph
EOD

# srun_commands

module purge
module load leibniz/supported
module use /data/antwerpen/grp/astrucchem/EasyBuild/modules/centos8/broadwell/2020a
module load QuantumESPRESSO/7.1-intel-2020a-PERTURBO-2.0.2-hybrid-rt2605
srun pw.x -nd 1 -inp 195norm-cri.scf.in > 195norm-cri.scf.out
srun pp.x -nd 1 -inp 195norm-cri-ae.pp.in > 195norm-cri-ae.pp.out
module purge
module load leibniz/supported
module use /data/antwerpen/grp/astrucchem/EasyBuild/modules/centos8/broadwell/2020a
module load Critic2/git-5dda1f3-foss-2020a
critic2 < 195norm-cri.cri > 195norm-cri.cro
```

Figure 34: .slurm file of DFT calculation

In the output's folder of the calculation, the files usually considered in order to perform a DFT analysis are the .cro file that can be converted into a .csv file to build the table used for the evaluation of critical points with information about atom involved in the interaction, electron density, laplacian, ellipticity and curvature of the bond path; have sometimes been analysed the .vmd file in order to visualize shape of the bond path and the position of the critical point.

The XYZ calculation was performed to obtain the .xyz file (Fig.35), used as input file in NCI plot calculations.

```
#SBATCH --ntasks 28 --nodes 1 --cpus-per-task 1
#SBATCH --time 6:00:00
#SBATCH --job-name $name-xyz
#SBATCH --output /scratch/antwerpen/208/vsc20851/qe/stdout/stdout.%j.%x
#SBATCH --error /scratch/antwerpen/208/vsc20851/qe/stderr/stderr.%j.%x
#SBATCH --mail-type=all
#SBATCH --mail-user=filippo.vacchi@student.uantwerpen.be

mkdir -p /scratch/antwerpen/208/vsc20851/qe/$name-xyz
directory="/scratch/antwerpen/208/vsc20851/qe/$name-xyz"

cd \${SLURM_SUBMIT_DIR}

# copy_commands
cp $name-ae.cube $directory
cd \$directory

cat > $name-xyz.cri <<- EOD
CRYSTAL $name-ae.cube
WRITE $name.xyz
EOD

# srun_commands

module purge
module load leibniz/supported
module use /data/antwerpen/grp/astrucchem/EasyBuild/modules/centos8/broadwell/2020a
module load Critic2/git-5dda1f3-foss-2020a
critic2 < $name-xyz.cri > $name-xyz.cro
```

Figure 35: Slurm file of xyz calculation

The output of this calculation is a xyz file that can be elaborated with software programs as "VMD"[27] or "vesta"; the same file was modified to isolate the group of atoms or the molecule useful for NCI plot computational experiment.

Sometimes have been used the keyword "molmotif" followed by a number in order to consider two or more crystal cells, this was useful when the interaction we wanted to analyse did not involve the molecule in the centre of the crystal cell.

The isolated fragments and the cube file from DFT calculation were used as input for NCI plot calculations (Fig.36).

```
cd /data/antwerpen/208/vsc20851/qe
for file in $@
do

        name=$(echo $file | cut -f 1 -d '.')
        echo $name

        cat > $name.pp.slurm <<-EOF
        #!/bin/bash

#SBATCH --ntasks 28 --nodes 1 --cpus-per-task 1
#SBATCH --time 6:00:00
#SBATCH --job-name $name-nci
#SBATCH --output /scratch/antwerpen/208/vsc20851/qe/stdout/stdout.%j.%x
#SBATCH --error /scratch/antwerpen/208/vsc20851/qe/stderr/stderr.%j.%x
#SBATCH --mail-type=all
#SBATCH --mail-user=filippo.vacchi@student.uantwerpen.be

mkdir -p /scratch/antwerpen/208/vsc20851/qe/$name-nci
directory="/scratch/antwerpen/208/vsc20851/qe/$name-nci"

cd \${SLURM_SUBMIT_DIR}

# copy_commands
 cp $name-ae.cube $directory
 cp $name-1.xyz $directory
 cp $name-2.xyz $directory
cd \$directory

cat > $name-nci.cri <<- EOD
 CRYSTAL $name-ae.cube
 LOAD $name-ae.cube

nciplo
 ONAME $name-nci.s
 fragment $name-1.xyz
 fragment $name-2.xyz
 icrements 0.04
endnciplot
EOD

# srun_commands

module purge
module load leibniz/supported
module use /data/antwerpen/grp/astrucchem/EasyBuild/modules/centos8/broadwell/2020a
module load Critic2/git-5dda1f3-foss-2020a
critic2 < $name-nci.cri > $name-nci.cro
```

Figure 36: .slurm file of NCI plot calculation

From the output's folder have been considered the vmd file, the dat file, the dens.cube file and the grad.cupe file, using them is possible to visualize the interaction in software program as VMD, and in this way we can evaluate parameters as the shape, the distribution of the electron density and the atoms involved.

For all the NCI plot calculations have been used the keyword increments followed by a number that was setted at 0.04 bohr, it can be interpreted as the step lengths for the NCIPLOT grid in each direction.

5.3 Synthesis

Even if during the internship period were performed only computational experiments, in this section is described the generic synthesis of the structures, most of them have never been published, and for this reason is included a short resume of the synthesis. The synthesis of the collection of compounds was done following a wittig reaction[28] in order to obtain a library of structures.

In the image below (Fig.37) are sumarized the conditions and the reagents used for the reaction, changing the aldehydes used the last part is possible to obtain the collection of compounds.

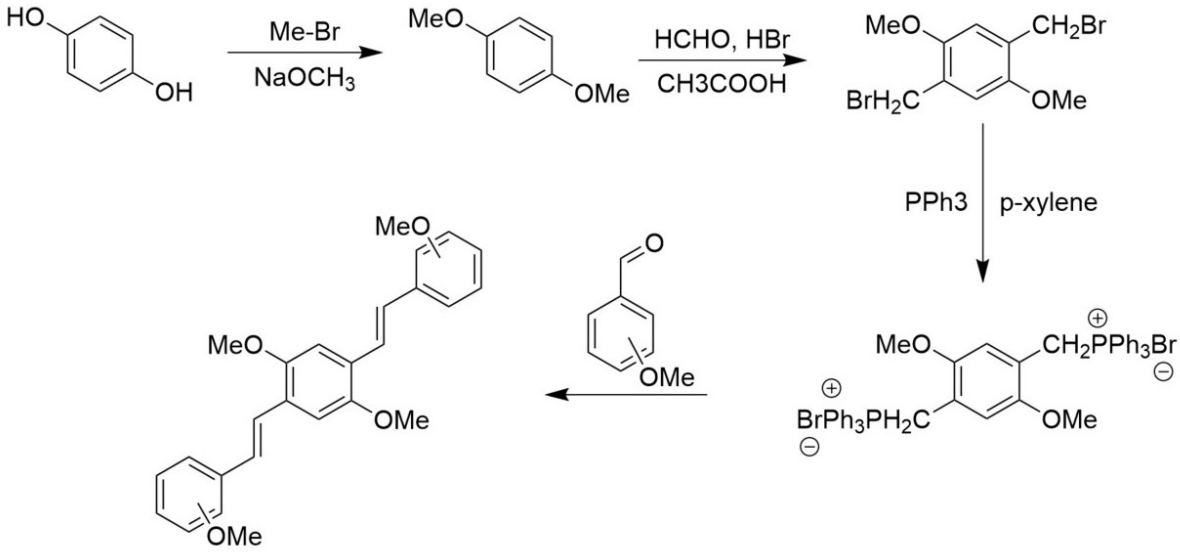

Figure 37: Synthetic pathways for the collection of compounds

All the molecules have been characterized with NMR.

5.4 XRD experiments and crystal detail

The XRD analysis of the collection of compounds was not carried on during the internship period, but the crystal data of 18 of 23 structures have never been published for this reason in order to complete the analysis is reported the procedure followed and the crystal data of structure [234MeO][25MeO] that was used for the NCI plot calculations (Tab.11).

The XRD experiments were executed on single crystals of [234MeO][25MeO]s.

Crystal data	
Chemical formula	$C_{30}H_{34}O_8$
Chemical formula weight g/mol	522.57
Cell settings	triclinic
Space group	P -1
Monochromator	Graphite
Crystal form	prism
Crystal size/mm	0.4 X 0.3 X 0.3
Crystal colour	Yellow
No. of reflection for cell param	25
θ Range/°	6.13-13.14
F(0 0 0)	278
T/K	293
a/Å	4.6950(10)
b/Å	7.053(2)
c/Å	20.121(4)
α/°	83.99(2)
β/°	88.66(2)
γ/°	87.19(2)
V/ Å^3	661.7(3)
Z	1
D_x/Mg m^{-3}	1.311
μ/mm^{-1}	0.095
Data collection method	omega/2theta scans
No. of measured reflections	4848
No. of independent reflections	2424
No. of observed reflections [I>2s(I)]	1817
Θ_{max}/°	25.30
Range of h	-5 ≤ h ≤ 5
Range of k	-8 ≤ k ≤ 8
Range of l	-24 ≤ l ≤ 24
No. of standard reflections	25
Frequency of standard reflections/h	1
Intensity decay (%)	1
Refinement on	F^2
GoOF	1.075
R_w	0.1308
R_u	0.03999
R_{all}	0.0606
No. of reflections used in refinement	2424
No. of parameters used	175
Weighting scheme	$w=1/[s^2 (Fo^2)+(0.0664P)^2+0.1715P]$ where $P=(Fo^2+2Fc^2)/3$
$(\Delta/\sigma)_{max}$	0
$\Delta\rho_{max}$	0.174
$\Delta\rho_{min}$	0.044

Table 11: Crystal data of molecule ***[234MeO][25MeO]***

The procedure described below is from a PHD thesis[20] of Blockhuys' research group.

Crystal structures of compounds [2MeO][], [246MeO][], [236MeO][], [23MeO][25MeO], [24MeO][25MeO], [234MeO][25MeO] and [236MeO][25MeO] were determined on an Enraf-Nonius Mach 3 diffractometer using Mo(Kα) radiation (λ= 0.71073 $\AA$) and w/2θ scans.

Structures of compounds [3MeO][], [23MeO][], [25MeO][], [26MeO][], [24MeO][], [34MeO][], [245MeO][], [234MeO][], [25MeO][25MeO], [26MeO][25MeO] and [34MeO][25MeO] were determined with a Bruker AXS SMART APEX CCD diffractometer using Mo(Kα) radiation (λ = 0.71073 $\AA$) and w scans; the data reduction and multiscan absorption correction was performed with the Apex2 v2008 2.4 software.

The structure of [25MeO][25MeO] was determined at 100 K because of the limited size of the crystal. A crystal of [34MeO][25MeO] proved to be a pseudo-merohedral twin (monoclinic but metrically orthorhombic) with a BASF of 0.216. The crystal of [234MeO][] under investigation was found to be non-merohedrally twinned.

The structures of [35MeO][], [345MeO][], [4MeO][25MeO], [246MeO][25MeO] and [345MeO][25MeO] were found on CSD database with ref code REDWUS, JACBIY, QORCEH, BEZYAH and GAKZAU.

References

[1] Arunachalam Ramanan Gautam R. Desiraju, Jagadese J. Vittal. Crystal engineering: A textbook. 2011.

[2] Dario Braga. Crystal engineering, where from? where to? *Chemical communications*, (22):2751–2754, 2003.

[3] Geetha Bolla, Bipul Sarma, and Ashwini K Nangia. Crystal engineering of pharmaceutical cocrystals in the discovery and development of improved drugs. *Chemical Reviews*, 122(13):11514–11603, 2022.

[4] Miranda L Cheney, Ning Shan, Elisabeth R Healey, Mazen Hanna, Lukasz Wojtas, Michael J Zaworotko, Vasyl Sava, Shijie Song, and Juan R Sanchez-Ramos. Effects of crystal form on solubility and pharmacokinetics: a crystal engineering case study of lamotrigine. *Crystal Growth & Design*, 10(1):394–405, 2010.

[5] Nicholas Blagden, Marcel de Matas, Pauline T Gavan, and Peter York. Crystal engineering of active pharmaceutical ingredients to improve solubility and dissolution rates. *Advanced drug delivery reviews*, 59(7):617–630, 2007.

[6] Christer B Aakeröy, Neil R Champness, and Christoph Janiak. Recent advances in crystal engineering. *CrystEngComm*, 12(1):22–43, 2010.

[7] AL Kitaigorodsky. *Molecular crystals and molecules*, volume 29. Elsevier, 2012.

[8] W Tachelet, S Jacobs, H Ndayikengurukiye, HJ Geise, and J Grüner. Blue electroluminescent devices with high quantum efficiency from alkoxy-substituted poly (para-phenylene vinylene)-trimers in a polystyrene matrix. *Applied physics letters*, 64(18):2364–2366, 1994.

[9] JP Yang, PL Heremans, R Hoefnagels, Wim Tachelet, P Dieltiens, F Blockhuys, HJ Geise, and Gustaaf Borghs. Blue organic light-emitting diode using 1, 4-bis (1, 1-diphenyl-2-ethenyl) benzene as an emitter. *Synthetic metals*, 108(2):95–100, 2000.

[10] Robert M Metzger, Bo Chen, Ulf Höpfner, MV Lakshmikantham, Dominique Vuillaume, Tsuyoshi Kawai, Xiangli Wu, Hiroaki Tachibana, Terry V Hughes, Hiromi Sakurai, et al. Unimolecular electrical rectification in hexadecylquinolinium tricyanoquinodimethanide. *Journal of the American Chemical Society*, 119(43):10455–10466, 1997.

[11] Robert M Metzger, Bo Chen, Ulf Höpfner, MV Lakshmikantham, Dominique Vuillaume, Tsuyoshi Kawai, Xiangli Wu, Hiroaki Tachibana, Terry V Hughes, Hiromi Sakurai, et al. Unimolecular electrical rectification in hexadecylquinolinium tricyanoquinodimethanide. *Journal of the American Chemical Society*, 119(43):10455–10466, 1997.

[12] James N Wilson and Uwe HF Bunz. Switching of intramolecular charge transfer in cruciforms: metal ion sensing. *Journal of the American Chemical Society*, 127(12):4124–4125, 2005.

[13] Masao Nohara, Masaki Hasegawa, Chishio Hosokawa, Hiroshi Tokailin, and Tadashi Kusumoto. A new series of electroluminescent organic compounds. *Chemistry Letters*, 19(2):189–190, 1990.

[14] Alain Collas, Izabela Bagrowska, Krzysztof Aleksandrzak, Matthias Zeller, and Frank Blockhuys. Competition between methoxy-based and pyrazine-based synthons in methoxy-substituted distyrylpyrazines. *Crystal Growth & Design*, 11(4):1299–1309, 2011.

[15] Chérif F. Matta, Jesús Hernández-Trujillo, Ting-Hua Tang, and Richard F. W. Bader. Hydrogen–hydrogen bonding: A stabilizing interaction in molecules and crystals. *Chemistry – A European Journal*, 9(9):1940–1951, 2003.

[16] Jordi Poater, Miquel Solà, and F. Matthias Bickelhaupt. Hydrogen–hydrogen bonding in planar biphenyl, predicted by atoms-in-molecules theory, does not exist. *Chemistry – A European Journal*, 12(10):2889–2895, 2006.

[17] Richard FW Bader. Pauli repulsions exist only in the eye of the beholder. *Chemistry–A European Journal*, 12(10):2896–2901, 2006.

[18] Jordi Poater, Miquel Solà, and F Matthias Bickelhaupt. A model of the chemical bond must be rooted in quantum mechanics, provide insight, and possess predictive power. *Chemistry–A European Journal*, 12(10):2902–2905, 2006.

[19] Richard FW Bader and TT Nguyen-Dang. Quantum theory of atoms in molecules–dalton revisited. In *Advances in Quantum Chemistry*, volume 14, pages 63–124. Elsevier, 1981.

[20] Alain Collas Frank Blockhuys. Molecular and crystal engineering: Asymmetric oligomers for polar crystals. 2011.

[21] Daniel GA Smith, Lori A Burns, Konrad Patkowski, and C David Sherrill. Revised damping parameters for the d3 dispersion correction to density functional theory. *The journal of physical chemistry letters*, 7(12):2197–2203, 2016.

[22] Stefan Grimme, Jens Antony, Stephan Ehrlich, and Helge Krieg. A consistent and accurate ab initio parametrization of density functional dispersion correction (dft-d) for the 94 elements h-pu. *The Journal of chemical physics*, 132(15), 2010.

[23] Stefan Grimme, Stephan Ehrlich, and Lars Goerigk. Effect of the damping function in dispersion corrected density functional theory. *Journal of computational chemistry*, 32(7):1456–1465, 2011.

[24] John P. Perdew, Kieron Burke, and Matthias Ernzerhof. Generalized gradient approximation made simple. *Phys. Rev. Lett.*, 77:3865–3868, Oct 1996.

[25] Zhigang Wu and R. E. Cohen. More accurate generalized gradient approximation for solids. *Phys. Rev. B*, 73:235116, Jun 2006.

[26] Pragya Verma and Donald G Truhlar. Status and challenges of density functional theory. *Trends in Chemistry*, 2(4):302–318, 2020.

[27] William Humphrey, Andrew Dalke, and Klaus Schulten. Vmd: visual molecular dynamics. *Journal of molecular graphics*, 14(1):33–38, 1996.

[28] Jan K Baeke, Jacek Nowaczyk, Maarten Moens, Li-Juan Chen, Pieter Dieltiens, Herman J Geise, Christian Van Alsenoy, and Frank Blockhuys. The electrochemistry of alkoxylated arylene vinylene oligomers: Oxidation potentials and diffusion coefficients. *Journal of Electroanalytical Chemistry*, 599(1):1–11, 2007.